

Highlights of Current Higgs Boson Searches

André Sopczak

Lancaster University

E-mail: andre.sopczak@cern.ch

ABSTRACT

Over the last years the Tevatron Run-II has extended several limits on Higgs boson masses and coupling which were pioneered during the LEP accelerator operation between 1989 and 2000. Higgs boson searches will also be at the forefront of research at the LHC. This review concisely discusses the experimental constraints set by the CDF and DØ collaborations in summer 2010 at the beginning of the LHC era. Model-independent and model-dependent limits on Higgs boson masses and couplings have been set and interpretations are discussed both in the Standard Model and in extended models. Recently, the Tevatron has extended the excluded SM Higgs boson mass range (158–175 GeV) beyond the LEP limit at 95% CL. The experimental sensitivities are estimated for the completion of the Tevatron programme.

*Contribution to the iNExT'10 conference
Sussex, UK, September 23–24, 2010*

1	Introduction	1
2	Production and Decay	1
3	b-Quark Tagging	3
4	Gluon Fusion $gg \rightarrow H \rightarrow WW$	4
5	Associated Production	4
5.1	$WH(H \rightarrow b\bar{b})$	4
5.2	$WH(H \rightarrow WW)$	6
5.3	$ZH \rightarrow \ell\ell b\bar{b}$	6
5.4	$ZH \rightarrow \nu\bar{\nu} b\bar{b}$	6
6	$H \rightarrow \tau^+\tau^-$	8
7	$H \rightarrow \gamma\gamma$	8
8	$t\bar{t}H$	9
9	Combined SM Higgs Boson Limits	9
10	Beyond the SM	11
10.1	$b\bar{b}h, b\bar{b}H, b\bar{b}A$	11
10.2	$h, H, A \rightarrow \tau^+\tau^-$	12
10.3	H^+	13
10.4	$H \rightarrow \gamma\gamma$	15
10.5	H^{++}	15
11	Conclusions	16

1. Introduction

The search for new particles is at the forefront of High Energy Physics. The discovery of a Higgs boson would shed light on electroweak symmetry breaking and the generation of mass in the Universe. Many searches for new particles were performed at LEP and stringent limits on Higgs bosons in the Standard Model (SM) and beyond were set, as summarized in Table 1 (from [1]) including model-independent LEP limits and benchmark results in the Minimal Supersymmetric extension of the SM (MSSM) [2]. In addition to the limits from direct searches, some indication on the Higgs boson mass exist from precision electroweak measurements, as shown in Fig. 1 (left and center plots from [3]). Up to 6.7 fb^{-1} of data have been analyzed so far (summer 2010) by each Tevatron experiment, which is about a 50% increase compared to the previous report [4] (winter 2008/9). This review is structured similar to the 2006 [5] and 2009 [4] reports to allow to compare more directly the experimental progress.

Both CDF and DØ have measured with precision various SM processes as illustrated in Fig. 1 (right plot from [6]). The figure includes also recent ZZ measurements [7, 8]. Figure 2 (from [9]) shows the delivered luminosity and its expectations.

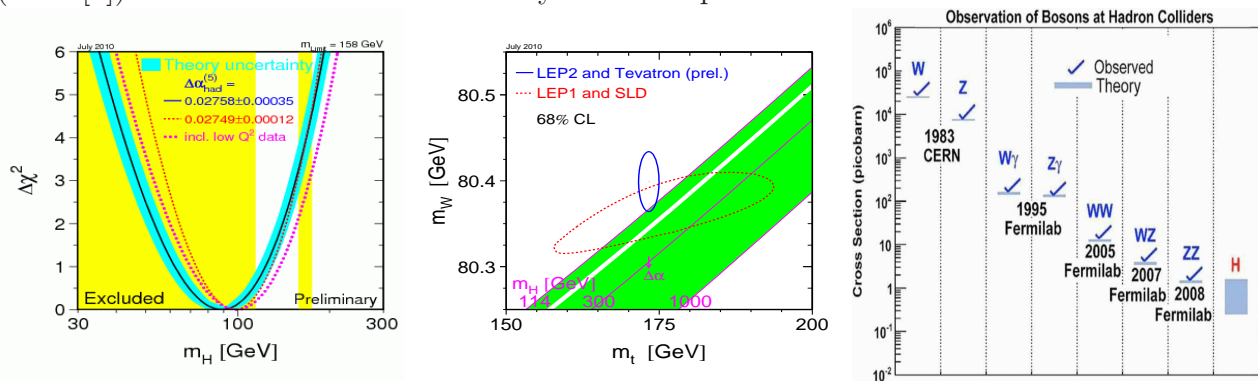


Figure 1. Left: Higgs boson mass prediction in the SM framework. The upper SM Higgs boson mass limit at 95% CL is 158 GeV. Center: smaller ellipse including LEP-2 and Tevatron data (solid line) prefers a region outside the SM Higgs boson mass band ($m_H = 114$ to 1000 GeV). The combined results from LEP-1 and SLD only are shown separately (dashed line). Right: overview of boson observations at hadron colliders, and indication of the expected cross-section for a SM Higgs boson.

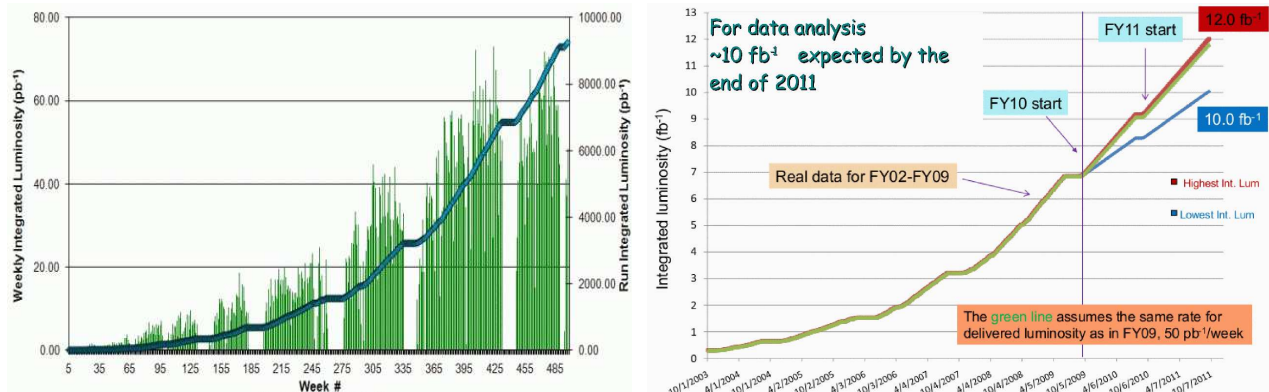


Figure 2. Left: integrated delivered Tevatron luminosity up to 17 September 2010. At the beginning of FY11 about 9 fb^{-1} are delivered, of which about 8 fb^{-1} are recorded and about 6 fb^{-1} are analysed. Right: expectation for future data-taking. The Tevatron has been operating on the higher luminosity slope.

2. Production and Decay

The expected cross-section and branching ratios are shown in Fig. 3 (from [10] and [11]) as a function of the Higgs boson mass. It is interesting to note that corresponding to the current

collected data sample of about 8 fb^{-1} about 8000 SM Higgs bosons of 120 GeV could have already been recorded in $p\bar{p}$ collisions at each experiment. For a SM Higgs boson mass below about 200 GeV the decay width is below 1 GeV which is much below the detector resolution.

Table 1. Summary of Higgs boson mass limits at 95% CL. ‘LEP’ indicates a combination of the results from ALEPH, DELPHI, L3 and OPAL. If results from the experiments are not (yet) combined, examples which represent the different search areas from individual experiments are given. Details are given in Ref. [1].

Search	experiment	limit
Standard Model	LEP	$m_H^{\text{SM}} > 114.4 \text{ GeV}$
Reduced rate and SM decay		$\xi^2 > 0.05 : m_H > 85 \text{ GeV}$
		$\xi^2 > 0.3 : m_H > 110 \text{ GeV}$
Reduced rate and $b\bar{b}$ decay		$\xi^2 > 0.04 : m_H > 80 \text{ GeV}$
		$\xi^2 > 0.25 : m_H > 110 \text{ GeV}$
Reduced rate and $\tau^+\tau^-$ decay		$\xi^2 > 0.2 : m_H > 113 \text{ GeV}$
Reduced rate and hadronic decay		$\xi^2 = 1 : m_H > 112.9 \text{ GeV}$
	ALEPH	$\xi^2 > 0.3 : m_H > 97 \text{ GeV}$
	L3	$\xi^2 > 0.04 : m_H \approx 90 \text{ GeV}$
Anomalous couplings		$d, d_B, \Delta g_1^Z, \Delta \kappa_\gamma$ exclusions
MSSM (no scalar top mixing)	LEP	almost entirely excluded
General MSSM scan	DELPHI	$m_h > 87 \text{ GeV}, m_A > 90 \text{ GeV}$
Larger top-quark mass	LEP	strongly reduced $\tan \beta$ limits
MSSM with CP-violating phases	LEP	strongly reduced mass limits
Visible/invisible Higgs decays	DELPHI	$m_H > 111.8 \text{ GeV}$
Majoron model (max. mixing)		$m_{H,S} > 112.1 \text{ GeV}$
Two-doublet Higgs model (for σ_{max})	DELPHI	$hA \rightarrow bbbb : m_h + m_A > 150 \text{ GeV}$ $\tau^+\tau^-\tau^+\tau^- : m_h + m_A > 160 \text{ GeV}$ $(AA)A \rightarrow 6b : m_h + m_A > 150 \text{ GeV}$ $(AA)Z \rightarrow 4b : m_h > 90 \text{ GeV}$ $hA \rightarrow q\bar{q}q\bar{q} : m_h + m_A > 110 \text{ GeV}$ $\tan \beta > 1 : m_h \approx m_A > 85 \text{ GeV}$
Two-doublet model scan	OPAL	
Yukawa process	DELPHI	$C > 40 : m_{h,A} > 40 \text{ GeV}$
Singly-charged Higgs bosons	LEP	$m_{H^\pm} > 78.6 \text{ GeV}$
$W^\pm A$ decay mode	DELPHI	$m_{H^\pm} > 76.7 \text{ GeV}$
Doubly-charged Higgs bosons	DELPHI/OPAL	$m_{H^{++}} > 99 \text{ GeV}$
$e^+e^- \rightarrow e^+e^-$	L3	$h_{ee} > 0.5 : m_{H^{++}} > 700 \text{ GeV}$
Fermiophobic $H \rightarrow WW, ZZ, \gamma\gamma$	L3	$m_H > 108.3 \text{ GeV}$
$H \rightarrow \gamma\gamma$	LEP	$m_H > 109.7 \text{ GeV}$
Uniform and stealthy scenarios	OPAL	depending on model parameters

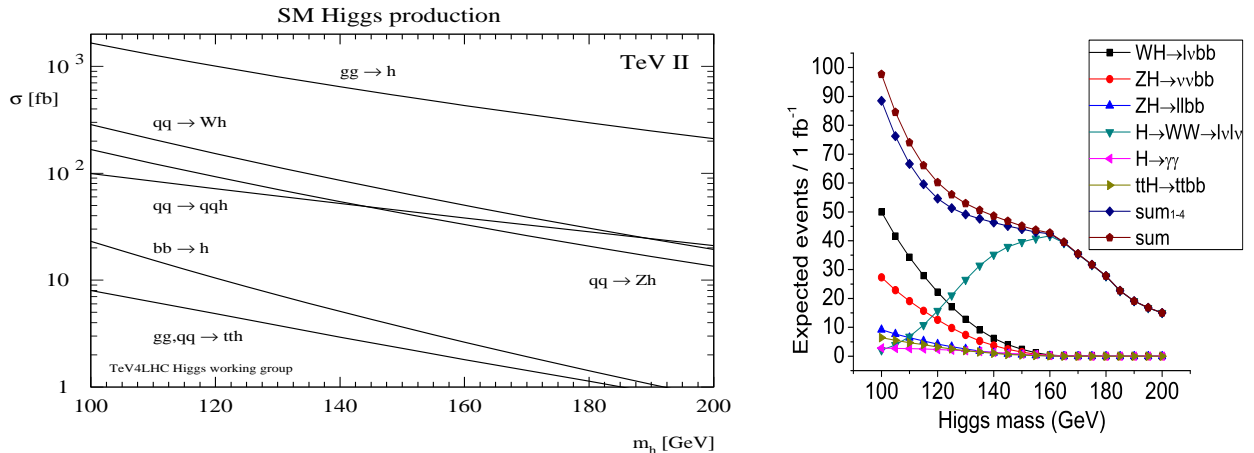


Figure 3. Left: expected SM Higgs boson production cross-sections at the Tevatron (1.96 TeV). Right: expected number of Higgs bosons (cross-section times decay branching ratios) for a SM Higgs boson.

3. b-Quark Tagging

The b-tagging capabilities are most important for the low-mass Higgs boson searches and a critical parameter is the impact parameter resolution of the vertex detector. The improvement of the impact parameter resolution with a sensitive layer very close to the interaction point is illustrated in Fig. 4 (left plot from [12] and center plot from [13]). In CDF this layer is called L00 and in $D\bar{O}$ it is called L0. These innermost layers contribute significantly to the b-tagging performance. Figure 4 (right plot from [14]) shows also the $D\bar{O}$ b-quark tagging performance including L0. An example of a quadruply b-tagged event is shown in Fig. 5 (from [15]).

Efficient B hadron tagging has already been demonstrated in data with $Z \rightarrow b\bar{b}$ events. These measurements contribute to the energy resolution and energy scale determinations. Figure 6 (left plot from [16], center plot from [17] and right plot from [18]) shows the reconstruction of the $Z \rightarrow b\bar{b}$ mass and the good agreement between data and simulation for b-tagged events.

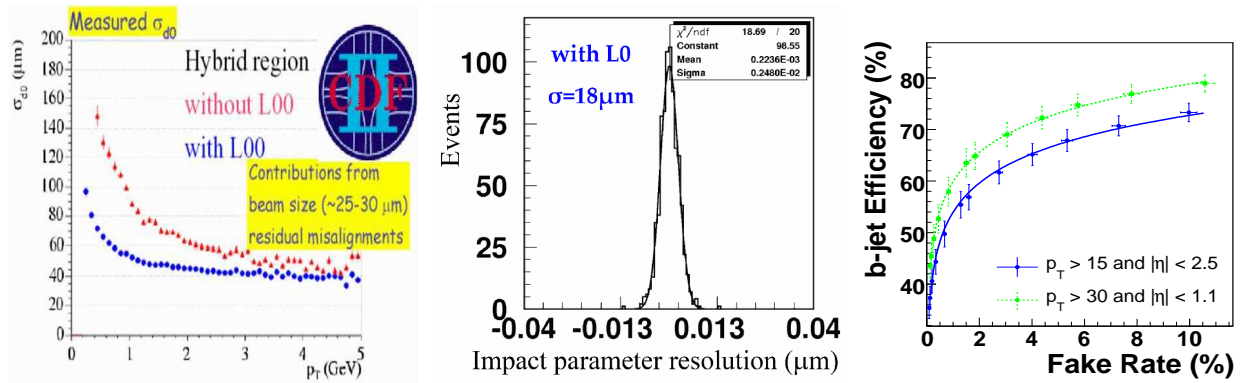


Figure 4. Left: CDF impact parameter resolution as a function of the transverse momentum p_T for tracks traversing passive material in vertex detector, with (blue dots) and without (red triangles) use of L00 hits. Center: $D\bar{O}$ impact parameter resolution after the installation of a new vertex detector layer (L0), which improved the resolution by 40%. Right: $D\bar{O}$ b-quark tagging performance for $Z \rightarrow b\bar{b}$ and $Z \rightarrow q\bar{q}$ events. The error bars include statistical and systematic uncertainties.

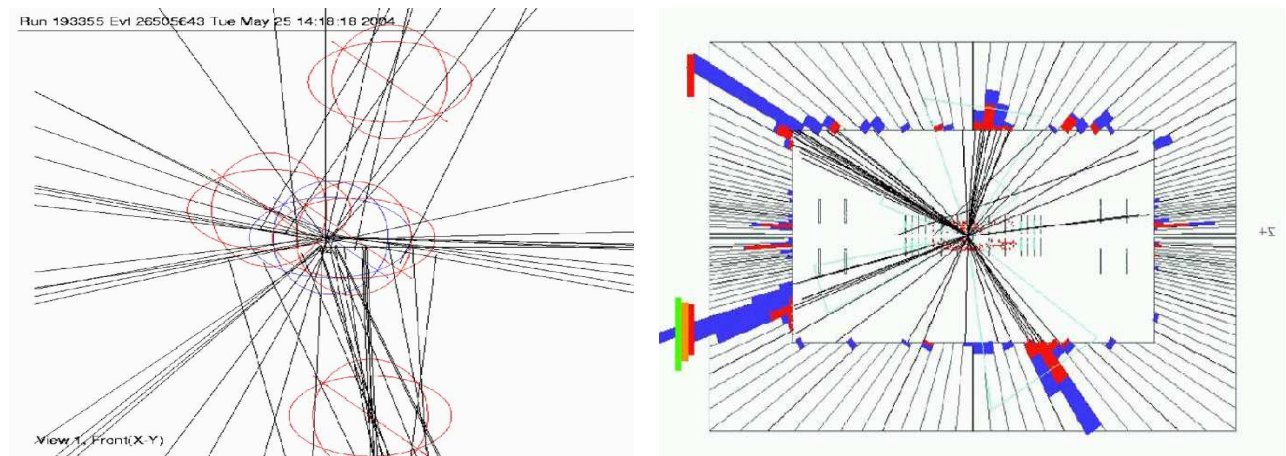


Figure 5. $D\bar{O}$ example of b-tagged event. Left: reconstructed tracks near the interaction point. Right: jets clearly visible in the calorimeter.

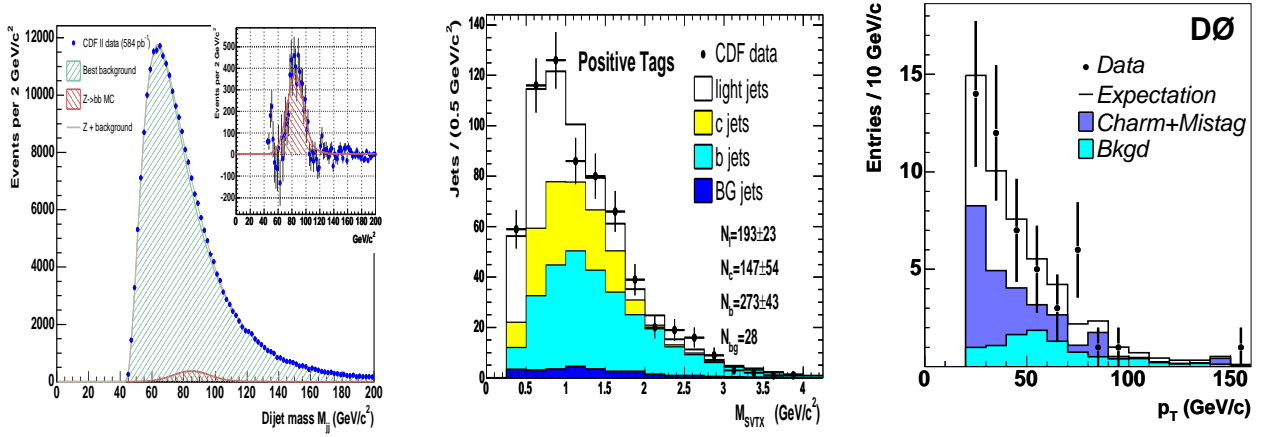


Figure 6. Left: CDF $Z \rightarrow b\bar{b}$ signal extracted in double-b-tagged data, relevant for $H \rightarrow b\bar{b}$ searches. Center: CDF invariant mass of tracks at the secondary vertex for positively tagged jets. Right: $D\bar{O}$ p_T distribution for b-tagged jets of Z+jets events.

4. Gluon Fusion $gg \rightarrow H \rightarrow WW$

For Higgs boson masses above about 135 GeV the process $gg \rightarrow H \rightarrow WW$ becomes important. The production and decay process is illustrated in Fig. 7, also shown is a background process leading to the same final state particles. The spin information allows separation of signal and background. The angle between the opposite charged leptons $\Delta\Phi_{ll}$ tends to be smaller for the signal than for the background as shown in Fig. 7 (from [19]). Based on 5.6–6.7 fb^{-1} total luminosity the neural network output for $gg \rightarrow H \rightarrow WW$ process and limits are shown in Fig. 8 (from [20]) and based on 5.9 fb^{-1} in Fig. 9 (from [21]). Owing to the overwhelming $b\bar{b}$ background, the $gg \rightarrow H(H \rightarrow b\bar{b})$ channel is not feasible at the Tevatron.

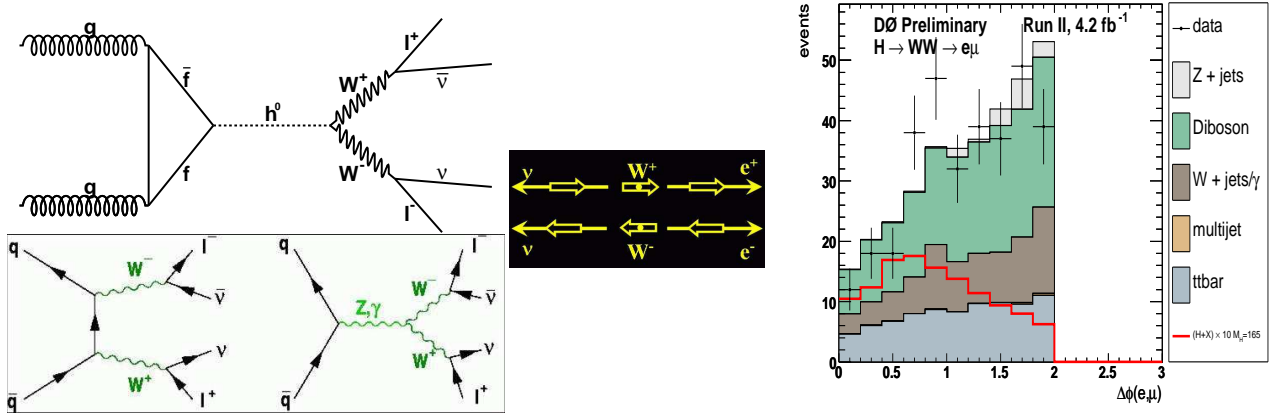


Figure 7. Left: $gg \rightarrow H(H \rightarrow WW)$ signal and background processes. Center: indication of spin correlations between final state leptons and W pairs, which lead to different dilepton azimuthal angular ($\Delta\Phi_{ll}$) distributions for signal and background. Right: $D\bar{O}$ $\Delta\Phi_{ll}$ distribution for data, and simulated signal and background. $\Delta\Phi_{ll}$ is predicted to be smaller for the signal.

5. Associated Production

5.1. $WH(H \rightarrow b\bar{b})$

An important discovery channel is the reaction $WH(H \rightarrow b\bar{b})$, where the W decays either to $e\nu$ or $\mu\nu$. The tagging of two b-quarks improves the signal to background ratio as shown in Fig. 10 (from [22]) and Fig. 11 (from [23]).

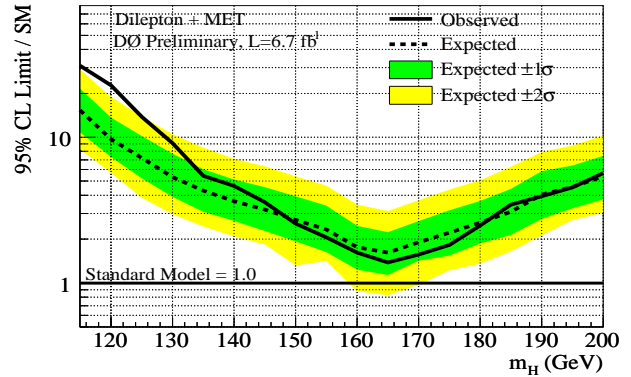
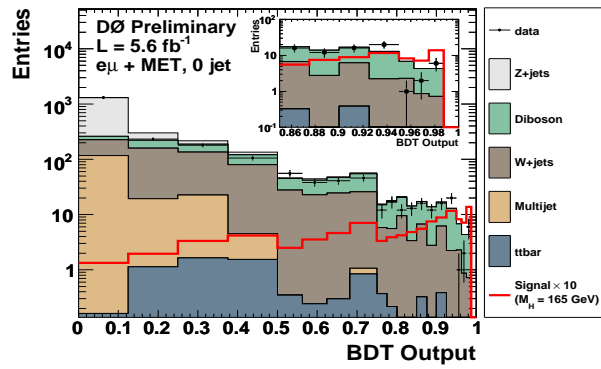


Figure 8. $D\bar{0} \text{ } gg \rightarrow H(H \rightarrow WW)$. Left: Boosted Decision Tree output. Right: limit at 95% CL ($e\mu$ channel only).

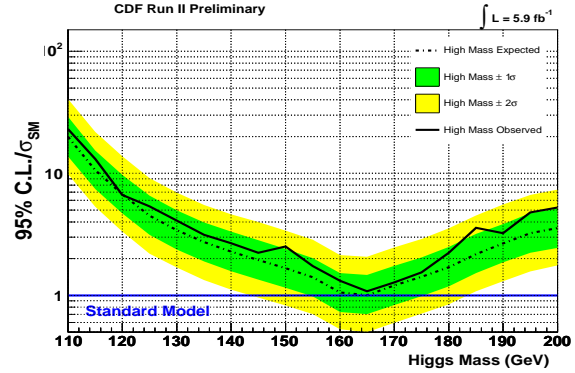
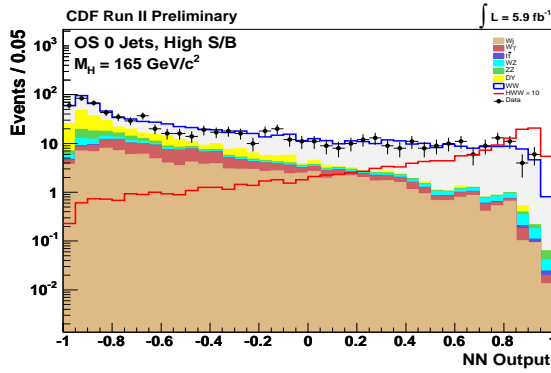


Figure 9. CDF $gg \rightarrow H(H \rightarrow WW)$. Left: Neural Network output. Right: limit at 95% CL ($e\mu$, e^+e^- and $\mu^+\mu^-$ channels combined) with $WH \rightarrow WWW$ and $ZH \rightarrow ZWW$ results.

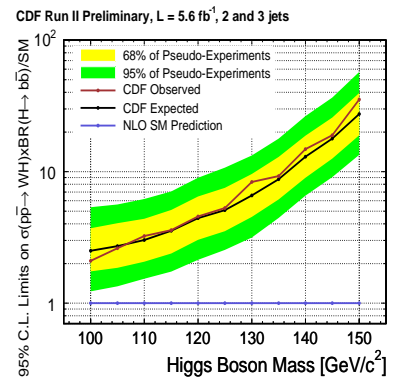
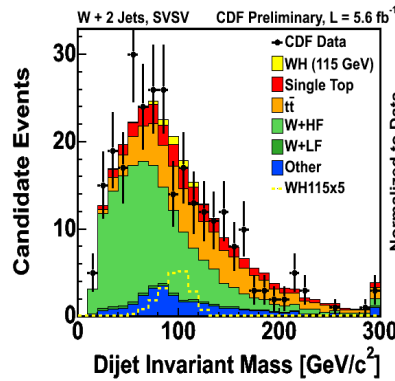
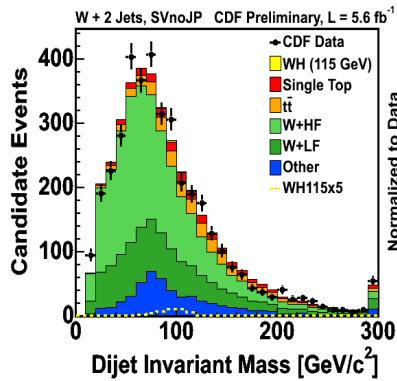


Figure 10. CDF $WH(H \rightarrow b\bar{b})$. Left: single b-tagging. Center: double b-tagging. Right: limit at 95% CL.

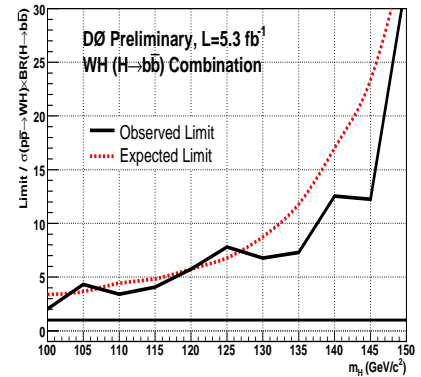
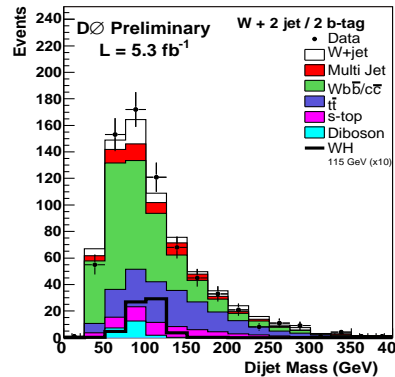
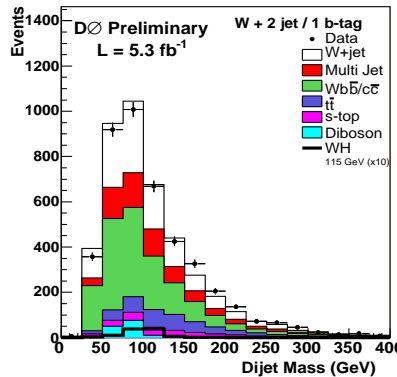


Figure 11. $D\bar{0} \text{ } WH(H \rightarrow b\bar{b})$. Left: single b-tagging. Center: double b-tagging. Right: limit at 95% CL.

5.2. WH($H \rightarrow WW$)

Results for the search WH($H \rightarrow WW$) in the tri-lepton and like-sign charged lepton final state are shown in Fig. 12 (from [21], 5.9 fb^{-1} luminosity) and Fig. 13 (from [24], 5.4 fb^{-1} luminosity). In the low-mass region this search channel has a weaker sensitivity as the $H \rightarrow b\bar{b}$ decay mode.

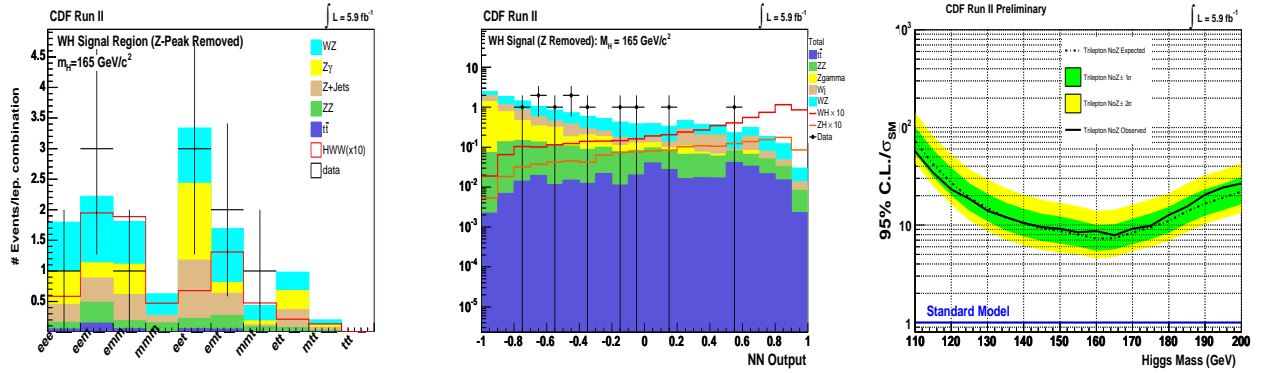


Figure 12. CDF WH($H \rightarrow WW$). Left: comparison of simulated background and observed number of events for electron, muon and taus tri-lepton events. Center: Neural network output. Right: limit at 95% CL.

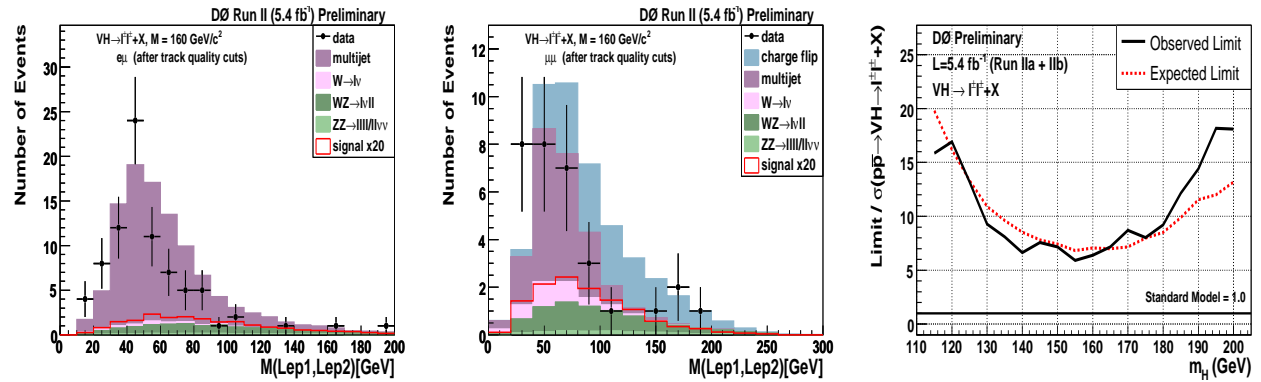


Figure 13. D0 WH($H \rightarrow WW$). Left: $e\mu$ invariant mass. Center: $\mu\mu$ invariant mass. Right: limit at 95% CL.

5.3. ZH $\rightarrow \ell\ell b\bar{b}$

The CDF and D0 collaborations have searched for ZH $\rightarrow e^+e^-b\bar{b}$ and $\mu^+\mu^-b\bar{b}$ signals. These signals are very clean, however, they have a small production cross-section. The results are shown in Fig. 14 (from [25]) and Fig. 15 (from [26]).

5.4. ZH $\rightarrow \nu\bar{\nu}b\bar{b}$

Both Tevatron collaborations have searched for a ZH $\rightarrow \nu\bar{\nu}b\bar{b}$ signal. The results from the expected missing energy and b-jet signal are shown in Fig. 16 (from [27]) and Fig. 17 (from [28]).

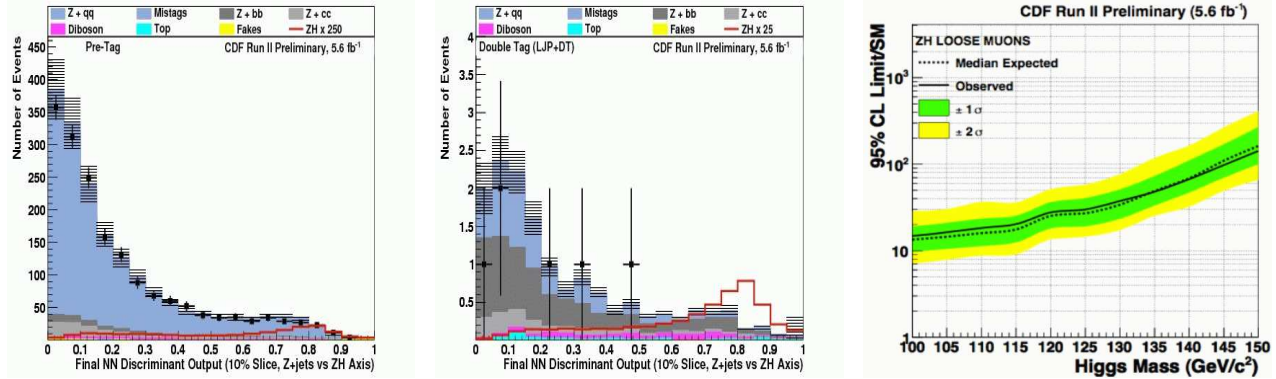


Figure 14. CDF $ZH(Z \rightarrow \ell\ell)(H \rightarrow b\bar{b})$. Left: $Z \rightarrow \ell^+\ell^-$ neural network output before b-quark tagging. Center: $Z \rightarrow \ell^+\ell^-$ neural network output after b-quark tagging. Right: limit at 95% CL.

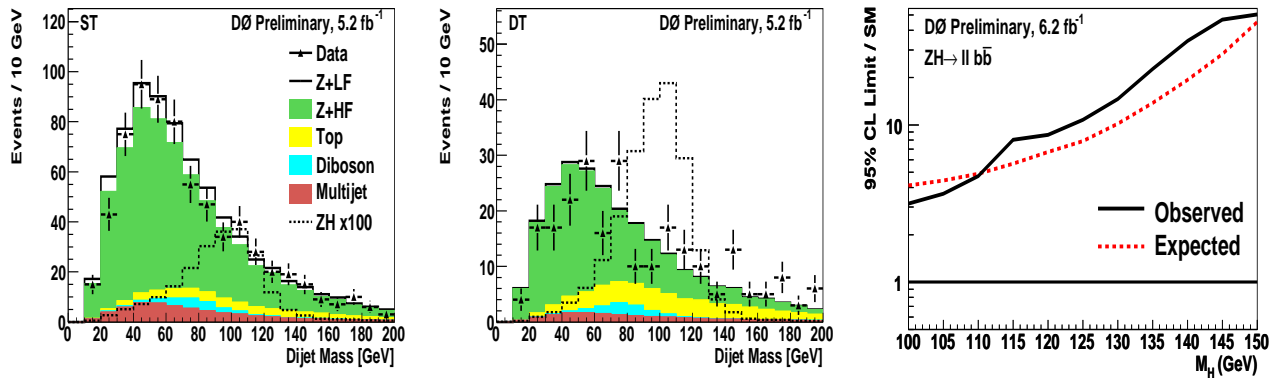


Figure 15. $D0 ZH(Z \rightarrow \ell\ell)(H \rightarrow b\bar{b})$. Left: invariant di-jet mass with single b-quark tagging. Center: invariant di-jet mass with double b-quark tagging. Right: limit at 95% CL.

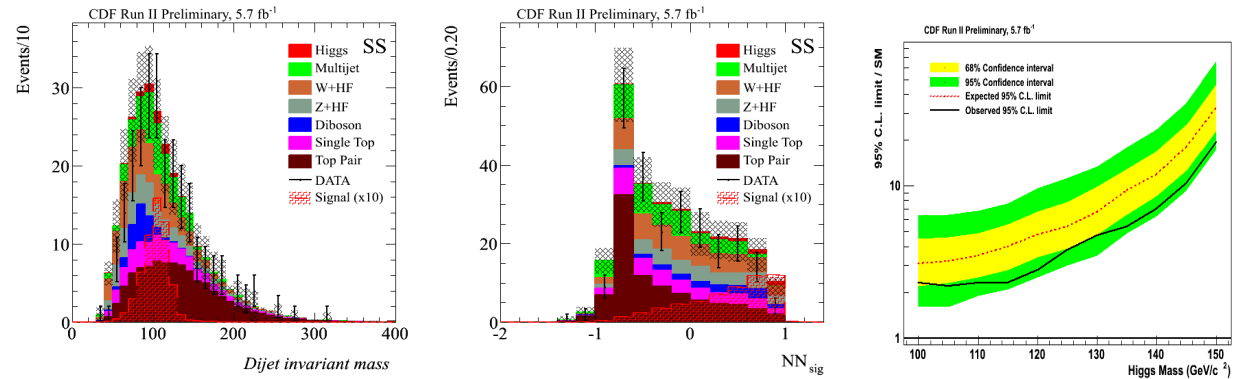


Figure 16. CDF $ZH(Z \rightarrow \nu\nu)(H \rightarrow b\bar{b})$. Left: invariant di-jet mass. Center: neural network output. Right: limit at 95% CL.

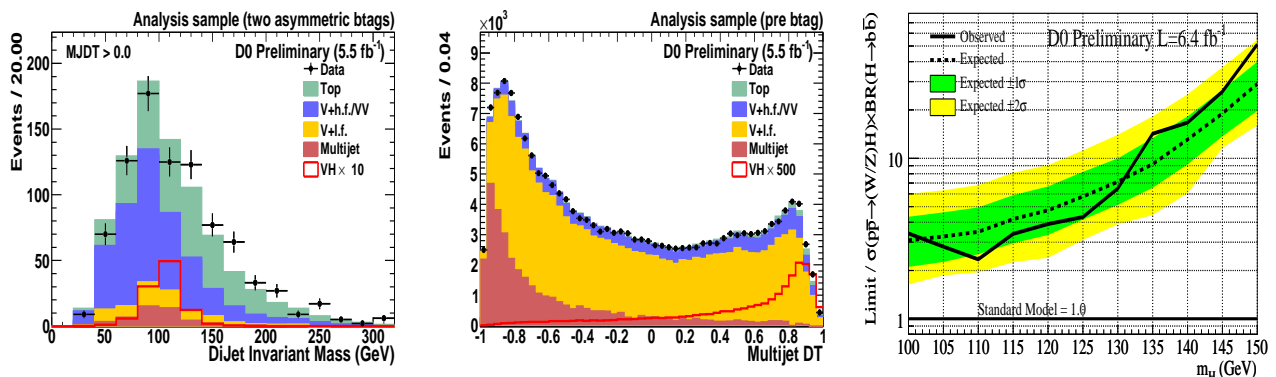


Figure 17. $D0 ZH(Z \rightarrow \nu\nu)(H \rightarrow b\bar{b})$. Left: invariant di-jet mass. Center: discriminant variable output. Right: limit at 95% CL.

6. $H \rightarrow \tau^+\tau^-$

Both Tevatron collaborations have searched for a $H \rightarrow \tau^+\tau^-$ signal. Results are shown in Figs. 18 (from [29]) and 19 (from [30]).

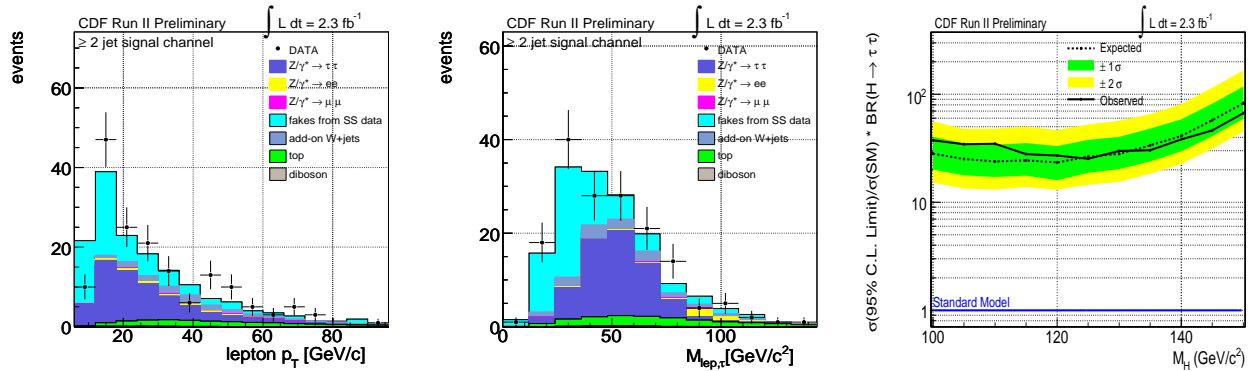


Figure 18. CDF ($H \rightarrow \tau^+\tau^-$). Left: lepton p_T . Center: invariant mass. Right: limit at 95% CL.

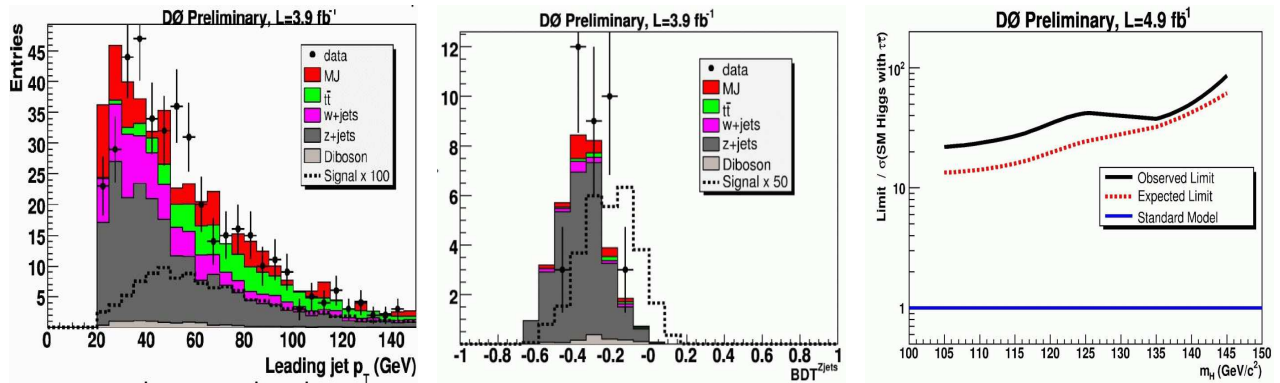


Figure 19. D0 ($H \rightarrow \tau^+\tau^-$). Left: leading p_T . Center: Boosted Decision Tree output. Right: limit at 95% CL.

7. $H \rightarrow \gamma\gamma$

Both Tevatron collaborations have searched for a $H \rightarrow \gamma\gamma$ signal. Results are shown in Figs. 20 (from [31]) and 21 (from [32]).

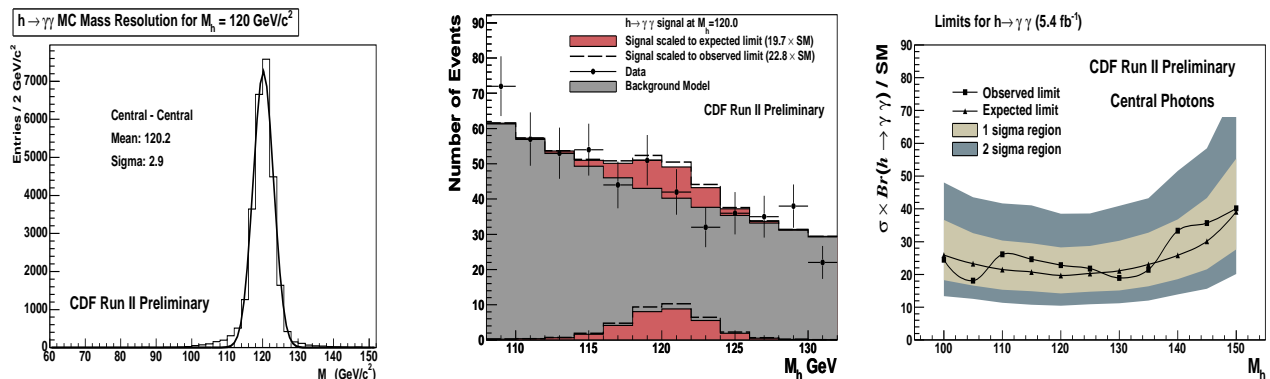


Figure 20. CDF ($H \rightarrow \gamma\gamma$). Left: simulated $H \rightarrow \gamma\gamma$ invariant mass. Center: invariant mass spectrum. Right: limit at 95% CL.

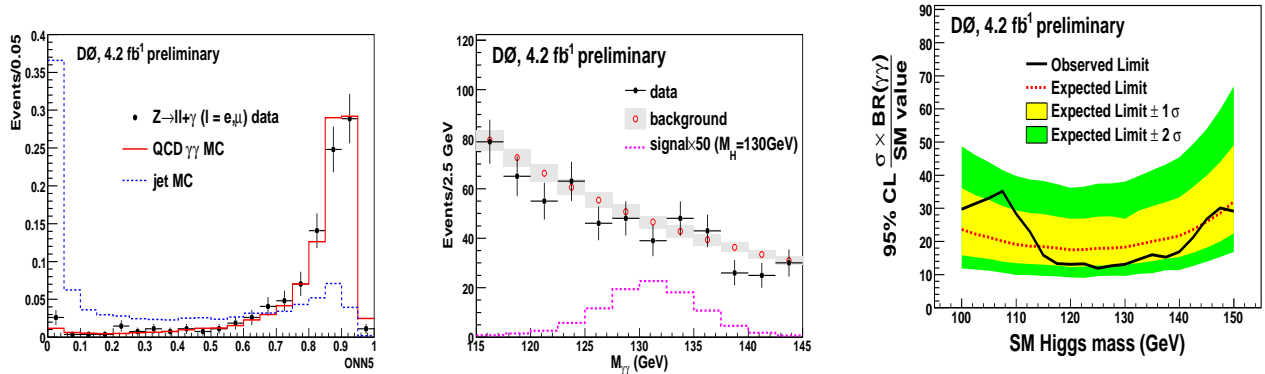


Figure 21. $D\bar{O}$ ($H \rightarrow \gamma\gamma$). Left: neural network output. Center: invariant mass. Right: limit at 95% CL.

8. $t\bar{t}H$

Both Tevatron collaborations have searched for a $t\bar{t} \rightarrow t\bar{t}H$ signal. Results are shown in Figs. 22 (from [33]) and 23 (from [34]).

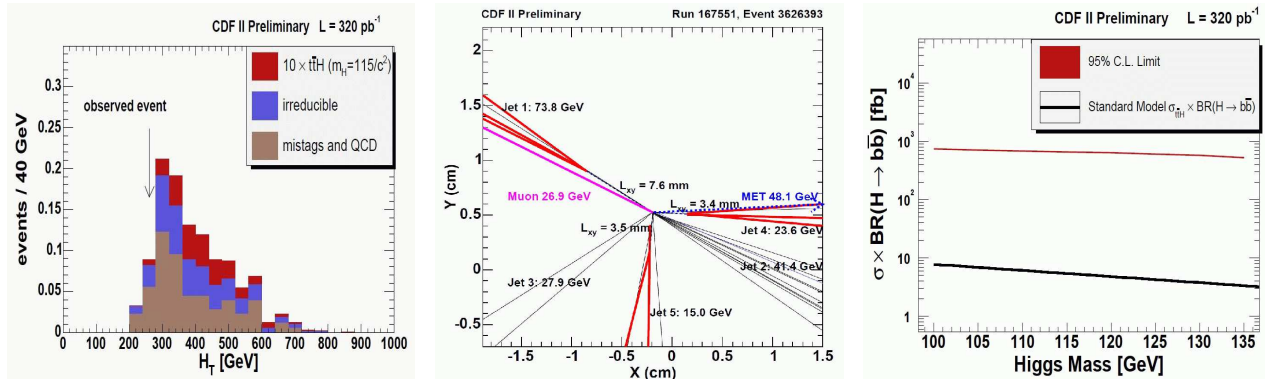


Figure 22. CDF ($t\bar{t} \rightarrow t\bar{t}H$). Left: H_T distribution. Center: candidate event. Right: limit at 95% CL.

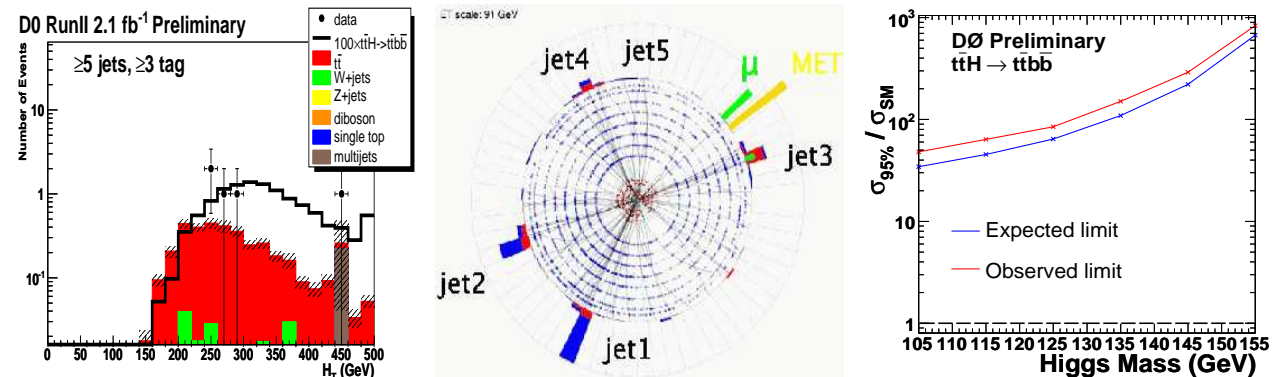


Figure 23. $D\bar{O}$ ($t\bar{t} \rightarrow t\bar{t}H$). Left: H_T distribution. Center: candidate event. Right: limit at 95% CL.

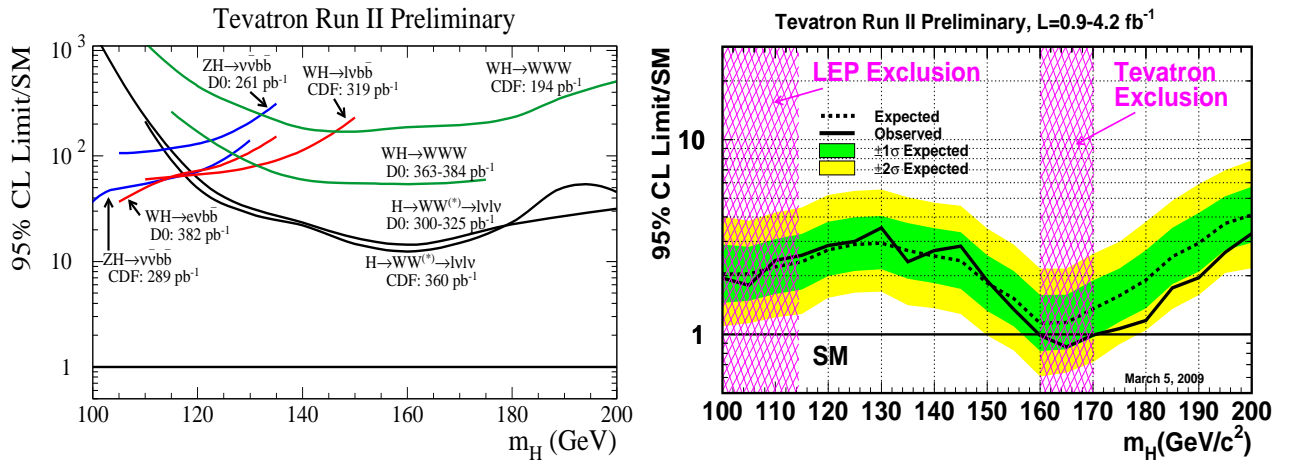
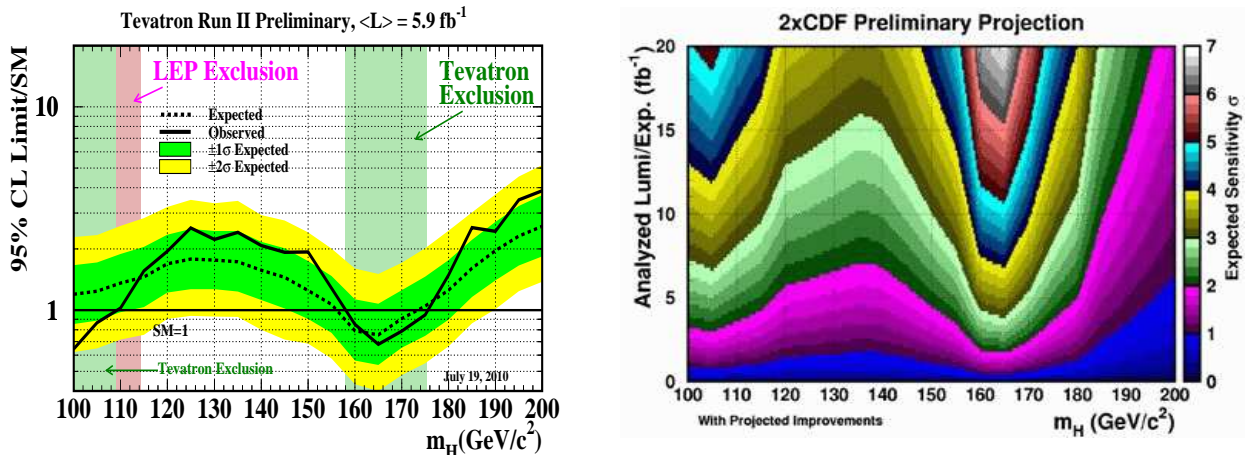
9. Combined SM Higgs Boson Limits

The large progress in sensitivity increase between results from summer 2005 (left plot from [5]) and combined CDF and $D\bar{O}$ results from winter 2008/9 (right plot from [35]) are shown in Fig. 24 with up to 4.2 fb^{-1} . Current limits with up to 6.7 fb^{-1} are shown in Fig. 25 (left plot from [36]). The achieved sensitivity in the various search channels is summarized in Table 2.

Improvements will continue to come from optimized b-quark tagging, and also from larger e/μ acceptance, better jet mass resolution, and from using advanced analysis techniques. Higher Higgs boson sensitivities will also result from the increase in luminosity. Currently (September 2010) about 9 fb^{-1} are delivered per experiment, and the total delivered luminosity could increase further up to about 17 fb^{-1} by the end of 2014. Resulting sensitivity estimates are shown in Fig. 25 (from [50]).

Table 2. Summary of observed and expected limits (where available) as factors compared to the SM expectation at 95% CL from CDF and DØ. The note numbers refer to CDF and DØ notes. (* $\epsilon\mu$ only)

Channel	Exper.	m_H (GeV)	\mathcal{L} (fb^{-1})	limit factor		Ref. note	\mathcal{L}_{new} (fb^{-1})	limit factor		Ref. note
				obs.	exp.			obs.	exp.	
$H \rightarrow WW \rightarrow \ell\nu\ell\nu$	CDF	160	3.6	1.5	1.5	9500 [38]	5.9	1.3	1.1	10232 [21]
	DØ	160	4.2	1.7	1.8	5871 [19]	6.7	*1.6	*1.8	6082 [20]
$WH \rightarrow \ell\nu b\bar{b}$	CDF	115	2.7	5.6	4.8	9596 [39]	5.7	3.6	3.5	10217 [22]
	DØ	115	2.7	6.7	6.4	5828 [40]	5.3	4.1	4.8	6092 [23]
W/ZH ($\rightarrow W/ZWW$)	CDF	160	2.7	25	20	7307 [41]	5.6	8.7	7.3	10232 [21]
	DØ	160	3.6	10	18	5873 [42]	5.4	6.4	7.1	6091 [24]
$ZH \rightarrow \ell\ell b\bar{b}$	CDF	115	2.7	7.1	9.9	9665 [43]	5.7	6.6	6.0	10235 [25]
	DØ	115	4.2	9.1	8.0	5876 [44]	6.2	8.0	5.7	6089 [26]
$ZH \rightarrow \nu\bar{\nu} b\bar{b}$	CDF	115	2.1	6.9	5.6	9642 [45]	5.7	2.3	4.0	10212 [27]
	DØ	115	2.1	7.5	8.4	5586 [46]	6.4	3.4	4.2	6087 [28]
W/ZH, VBF, ggH ($H \rightarrow \tau^+\tau^-$)	CDF	115	2.0	31	25	9248 [47]	2.3	27.9	24.5	10133 [29]
	DØ	115	1.0	27	28	5883 [48]	4.9	27.0	15.9	5845 [30]
$H \rightarrow \gamma\gamma$	CDF	–	3.0	–	–	9586 [49]	5.4	24.2	20.5	10065 [31]
	DØ	115	4.2	16	19	5858 [32]	–	–	–	unchanged
$t\bar{t}H$	CDF	–	0.3	–	–	9508 [33]	–	–	–	unchanged
	DØ	115	2.1	64	45	5739 [34]	–	–	–	unchanged
$W/ZH \rightarrow jj b\bar{b}$	CDF	115	–	–	–	–	4.0	9.1	17.8	10010 [37]


Figure 24. Comparison of progress between summer 2005 and winter 2008/9. Left: ratio of observed cross-section limit and expected SM cross-section, status summer 2005. Right: combined CDF and DØ limits at 95% CL, status winter 2008/9. Note that a region between 160 and 170 GeV mass is excluded.

Figure 25. Left: current combined CDF and DØ limits at 95% CL, status summer 2010. Note that a region between 158 and 175 GeV mass is excluded. Right: outlook for a mass range between 100 to 200 GeV.

10. Beyond the SM

10.1. $b\bar{b}h$, $b\bar{b}H$, $b\bar{b}A$

Higgs boson production processes in association with b-quarks in $p\bar{p}$ collisions have been calculated in two ways: in the five-flavor scheme [51], where only one b-quark has to be present in the final state, while in the four-flavor scheme [52], two b-quarks are explicitly required in the calculation. Both calculations are available at next-to-leading order (NLO QCD), and agree taking into account the theoretical uncertainties. Figure 26 (left plot from [53]) illustrates these processes for h production at leading order (LO), and analogous diagrams can be drawn for the H and A bosons. The cross-section depends on $\tan^2 \beta$ and on other Supersymmetric parameters as given by $\sigma \times BR_{\text{SUSY}} \approx 2\sigma_{\text{SM}} \tan^2 \beta / (1 + \delta_b)^2 \times 9 / (9 + (1 + \delta_b)^2)$, where $\delta_b = k \tan \beta$ with k depending on the SUSY parameters, in particular also on A_t , the mixing in the scalar top sector, the gluino mass, the μ parameter, stop and sbottom masses. The dependence of the production cross-section enhancement factor on $\tan \beta$ is shown in Fig. 26 (right plot from [53]). At tree-level the production cross-section rises with $\tan^2 \beta$.

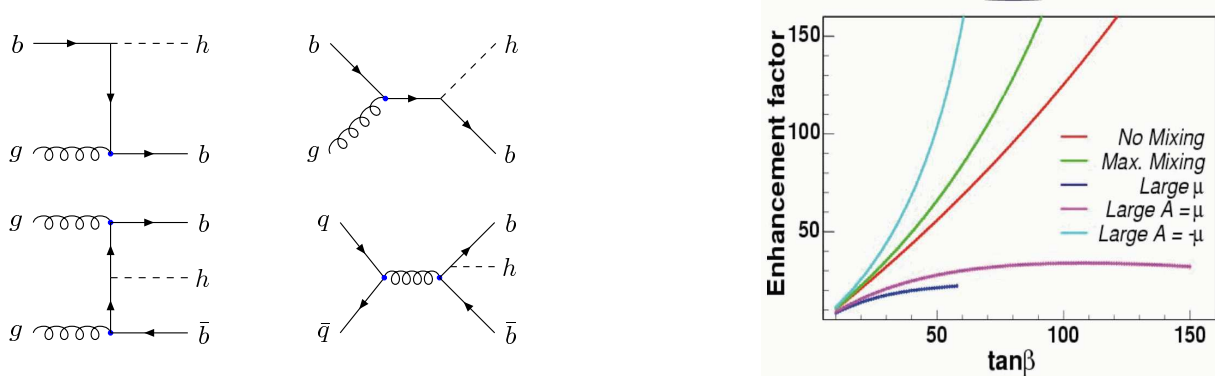


Figure 26. DØ. Left: leading-order Feynman diagrams for neutral Higgs boson production in the five-flavor scheme (top) and four-flavor scheme (bottom). Right: enhancement factor as a function of $\tan \beta$.

There is no indication of a $b\bar{b}A$ production in the data. Results from CDF and DØ are shown in Fig. 27 (from [54]) and Fig. 28 (from [55]). In the CDF results based on 1.9 fb^{-1} data statistical and systematic errors contribute about equally, therefore, with about 8 fb^{-1} data, cross-section sensitivities could be improved by about 20%, thus $\tan \beta$ sensitivities by about 10%. Estimates reported in 2005 [5] were too optimistic.

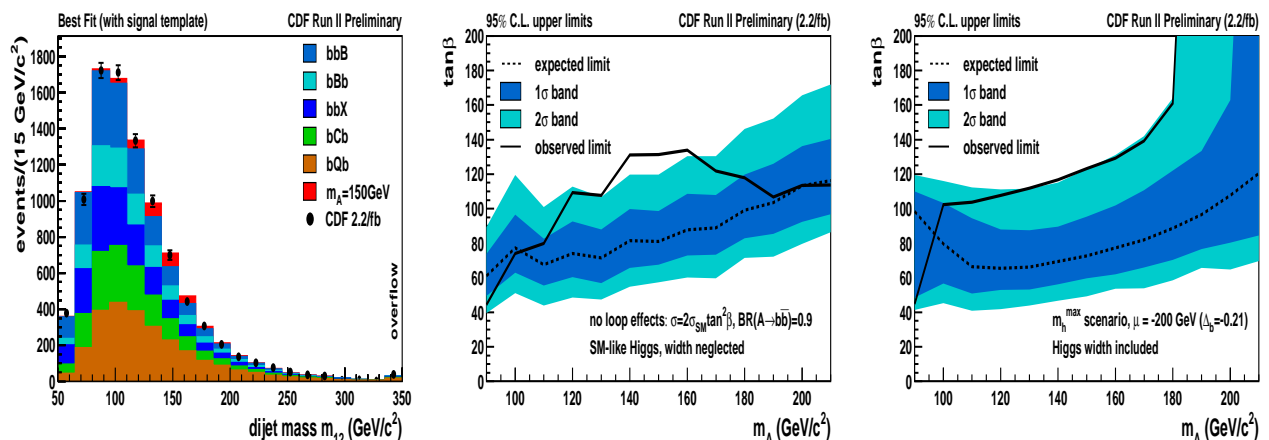


Figure 27. CDF $b\bar{b}A$ ($A \rightarrow b\bar{b}$). Left: invariant mass of the two most energetic jets $m_A = 150 \text{ GeV}$. Center: limits on $\tan \beta$ in the general Two Higgs Doublet Model (THDM). Right: limits on $\tan \beta$ in the MSSM for the m_h^{max} scenario.

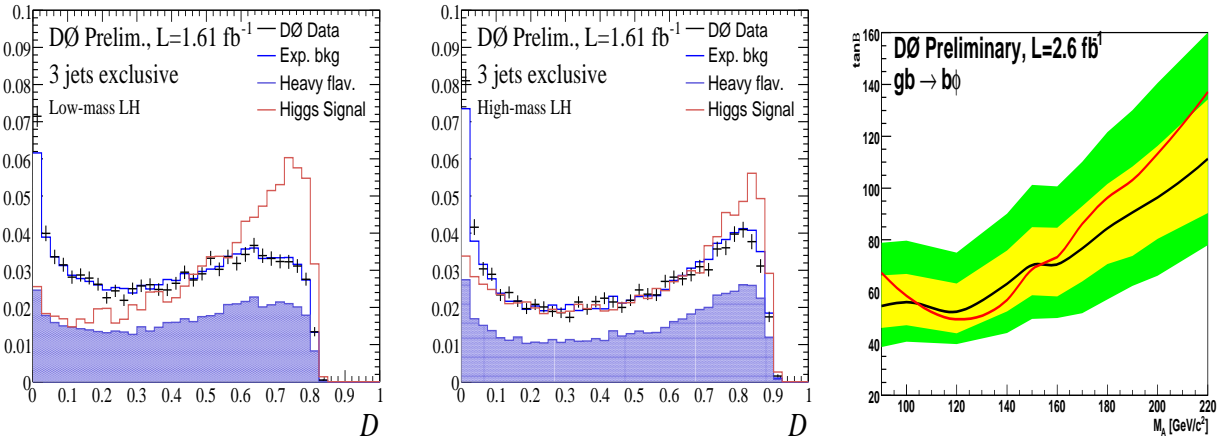


Figure 28. DØ $b\bar{b}(A \rightarrow b\bar{b})$. Left: discriminant variable output, low-mass. Center: discriminant variable output, high-mass. Right: limit at 95% CL.

10.2. $h, H, A \rightarrow \tau^+\tau^-$

The signature for $h, H, A \rightarrow \tau^+\tau^-$ opens additional possibilities for a Higgs boson discovery. Results from CDF and DØ are shown in Fig. 29 (from [56]) and Fig. 30 (left plot from [57]) and combined CDF and DØ results (center and right plots from [58]).

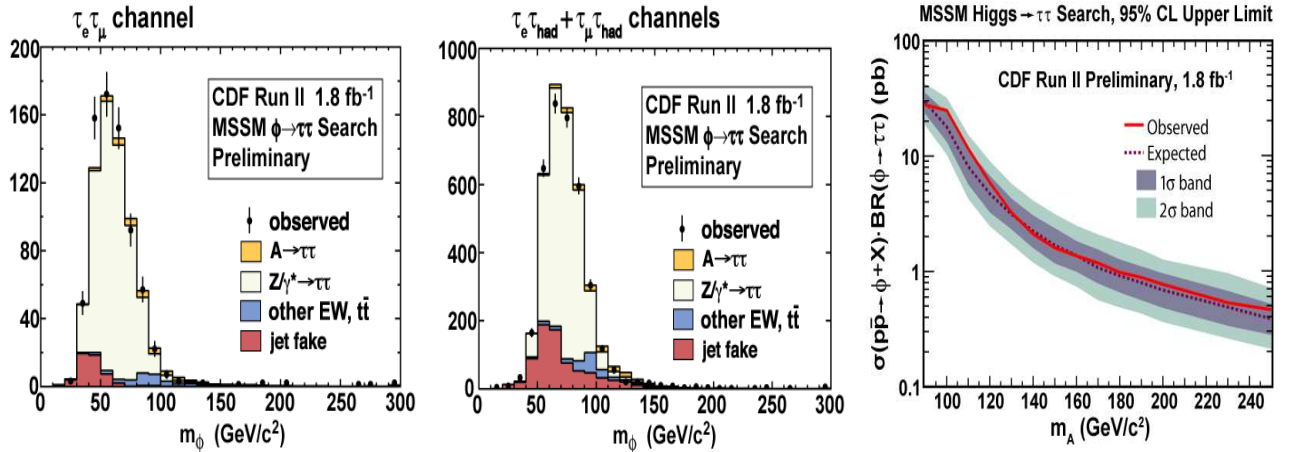


Figure 29. CDF. Left: invariant mass $e\mu$ channel for $\Phi = A$ with $m_A = 140$ GeV. Center: invariant mass $\ell\tau_h$ channel where ℓ represents an electron or a muon. Right: cross-section limit at 95% CL.

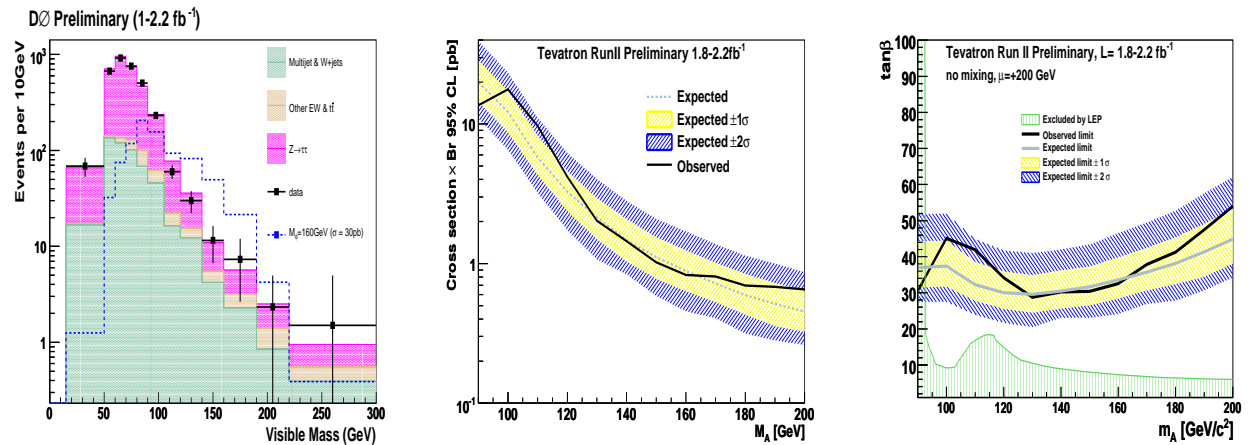


Figure 30. Left: DØ visible mass for $\Phi = A$ with $m_A = 160$ GeV. Center: combined CDF and DØ cross-section limit at 95% CL. Right: combined CDF and DØ MSSM limit at 95% CL.

10.3. H^+

The decay of top quarks $t \rightarrow H^+ b$ is possible in general Higgs boson models with two Higgs boson doublets. The expected top and charged Higgs boson branching fractions are shown in Fig. 31 (left plot from [59]) as a function of $\tan\beta$ for a specific MSSM parameter set. The expected SM top decay rate would be modified. No deviation from the SM top decay rates is observed. Results from CDF for 0.192 fb^{-1} are shown in Fig. 31 (right plot from [60]) and from DØ for 1 fb^{-1} are shown in Figs. 32 and 33 (from [59]).

An independent search has been carried out by DØ based on measuring the ratio $R = \sigma(t\bar{t})_{\ell+\text{jets}}/\sigma(t\bar{t})_{\ell+\ell^-}$ [61]. In the SM $R = 1$, while a decay $t \rightarrow H^+ b$ changes this ratio. Results are summarized in Fig. 34 (from [61]) for a leptophobic charged Higgs boson.

A charged Higgs boson search by CDF focuses on the reaction $t \rightarrow H^+ b$ ($H^+ \rightarrow c\bar{s}$) based on 2.2 fb^{-1} data [62]. The hadronic charged Higgs boson decay mode would allow a precise H^+ mass reconstruction. Results are summarized in Fig. 35 (from [62]).

In the high mass regime ($m_{H^+} > m_t$) the search for charged Higgs bosons has been performed similar as for the single top s-channel analysis with $\mathcal{L} = 0.9 \text{ fb}^{-1}$. The reaction is $q\bar{q}' \rightarrow H^+ \rightarrow t\bar{b} \rightarrow W^+ b\bar{b} \rightarrow \ell^+ \nu b\bar{b}$, where ℓ represents an electron or a muon [63]. Results are summarized in Fig. 36 (from [63]).

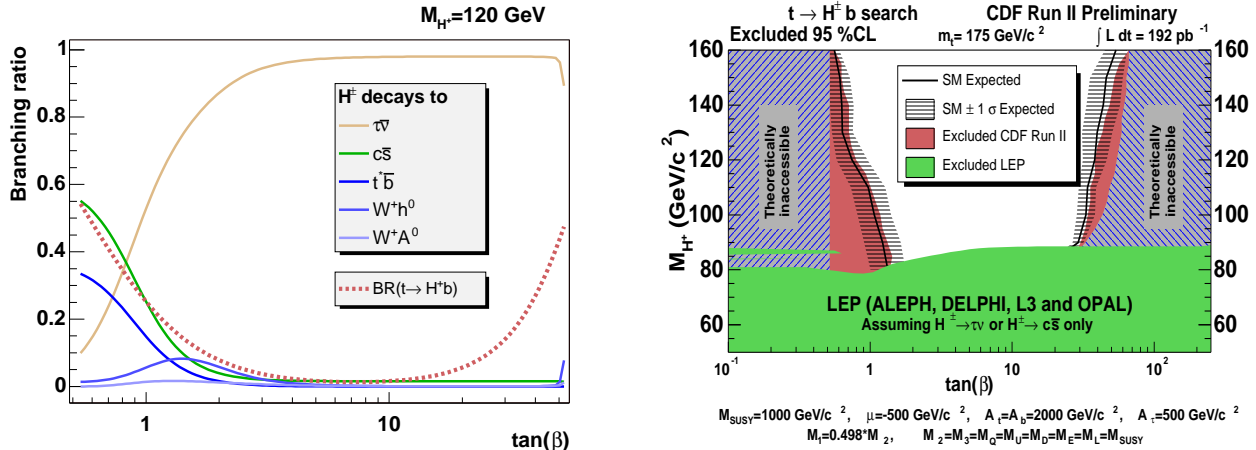


Figure 31. Left: branching ratios for a 120 GeV charged Higgs boson production in top decays and charged Higgs boson decays as a function of $\tan\beta$ in the MSSM. Right: CDF. Limits on the charged Higgs boson mass as function of $\tan\beta$ for a specific set of MSSM parameters.

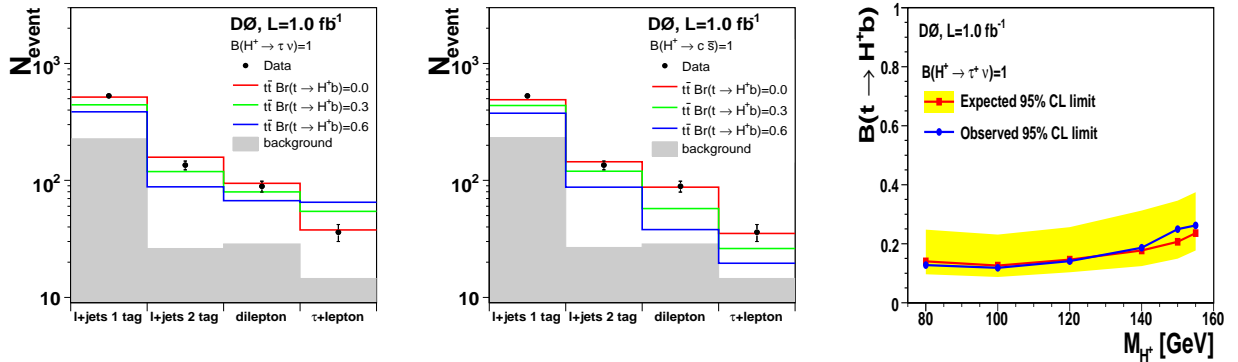


Figure 32. DØ. Left: variation of number of expected events for $t \rightarrow H^+ b$ ($H^+ \rightarrow \tau\nu$). Center: variation of number of expected events for $t \rightarrow H^+ b$ ($H^+ \rightarrow c\bar{s}$). Right: $BR(t \rightarrow H^+ b)$ limit at 95% CL for $BR(H^+ \rightarrow \tau\nu) = 1$.

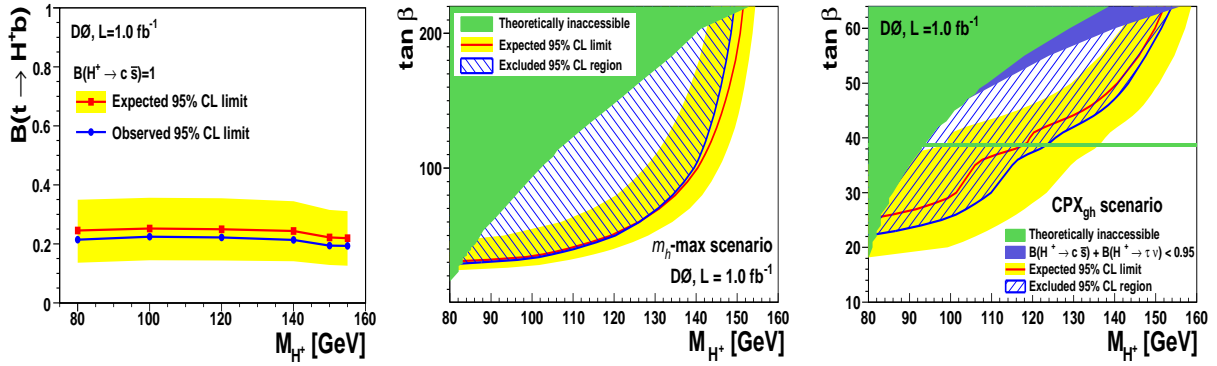


Figure 33. $D\emptyset$. Left: $\text{BR}(t \rightarrow H^+ b)$ limit at 95% CL for $\text{BR}(H^+ \rightarrow c\bar{s}) = 1$. Center: limits for a specific set (mhmax) of MSSM parameters. Right: limits for a specific set (CPX) of MSSM parameters.

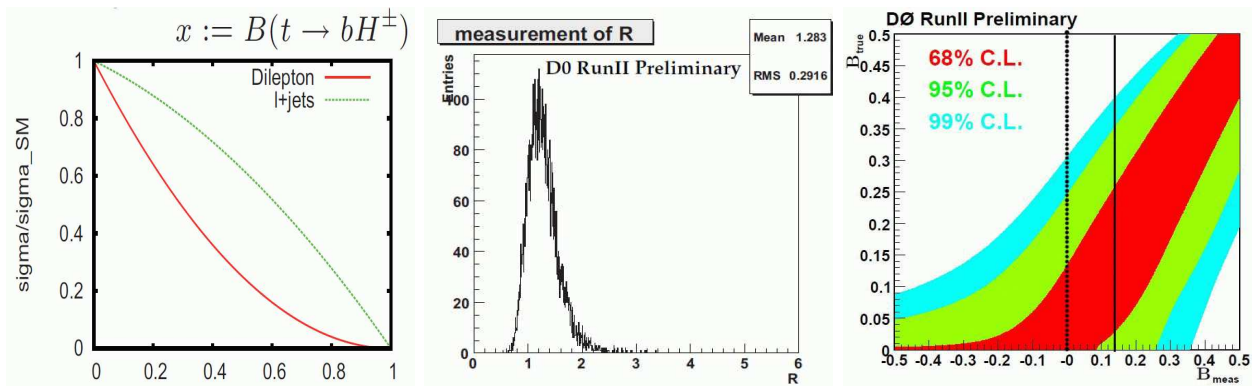


Figure 34. $D\emptyset$. Left: modified cross-sections relative to the SM cross-section as functions of $\text{BR}(t \rightarrow H^+ b)$. Center: distribution of cross-section ratio R generated from the 10,000 pseudo-experiments. Right: Feldman-Cousins confidence interval bands as functions of measured and generated branching fraction $\text{BR}(t \rightarrow H^+ b)$. For a leptophobic 80 GeV charged Higgs boson, $\text{BR}(H^+ \rightarrow c\bar{s})=1$, $\text{BR}(t \rightarrow H^+ b)$ limits at 95% CL are 0.35 (observed, solid line) and 0.25 (expected, dotted line).

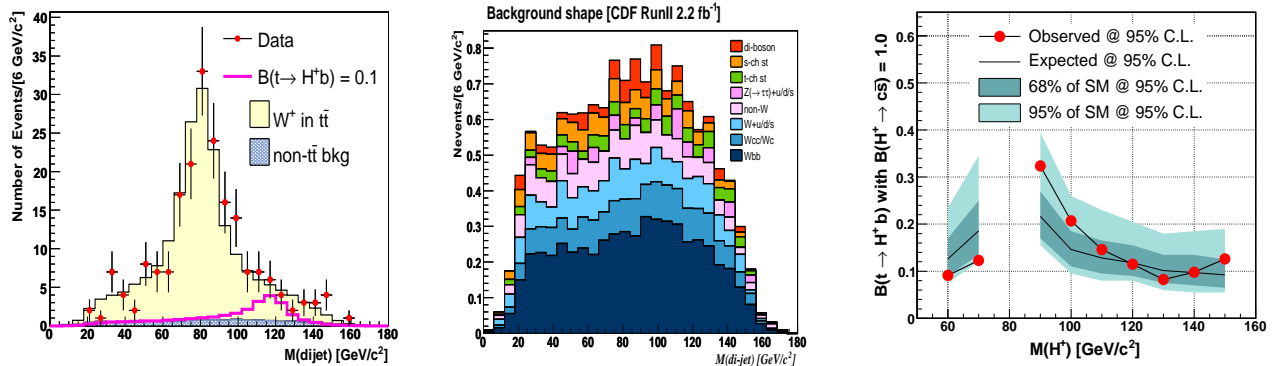


Figure 35. CDF. Left: di-jet mass in top decays. Center: background contributions to the di-jet mass in top decays. Right: model-independent $\text{BR}(t \rightarrow H^+ b)$ limit for $\text{BR}(H^+ \rightarrow c\bar{s}) = 1$. In order to cover any generic anomalous charged Higgs boson, the search is extended below the W mass.

In the Next-to-MSSM (NMSSM) a charged Higgs boson search by CDF has been performed in the reaction $t \rightarrow H^+ b \rightarrow W^+ A b$ ($A \rightarrow \tau^+ \tau^-$) based on 2.7 fb^{-1} data. The decay ($A \rightarrow \tau^+ \tau^-$) could be dominant as shown in Fig. 37 (left plot from [64]). Results are summarized in Fig. 37 (right and center plots from [65]).

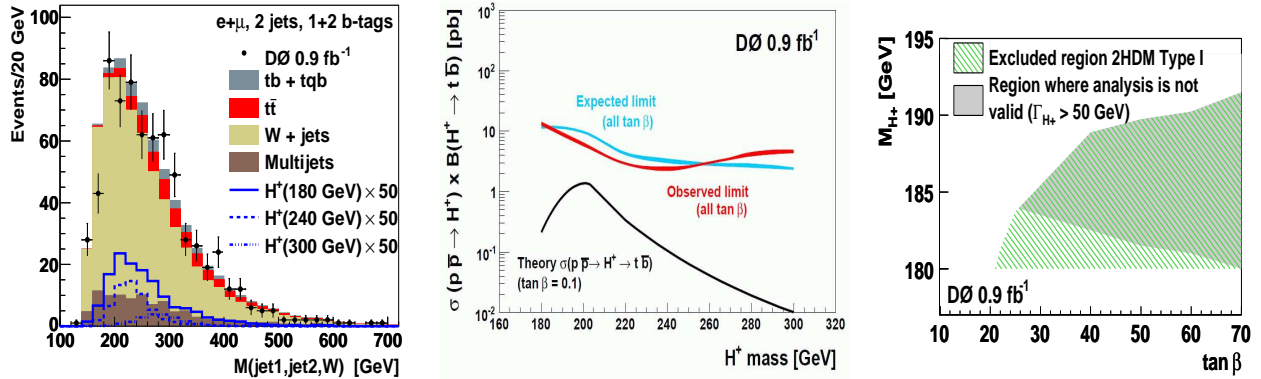


Figure 36. $D\bar{0} \text{ } p\bar{p} \rightarrow H^+ \rightarrow t\bar{b}$. Left: invariant charged Higgs boson mass (type III model). Center: cross-section limit in THDM (type II). Right: THDM excluded regions for model type I.

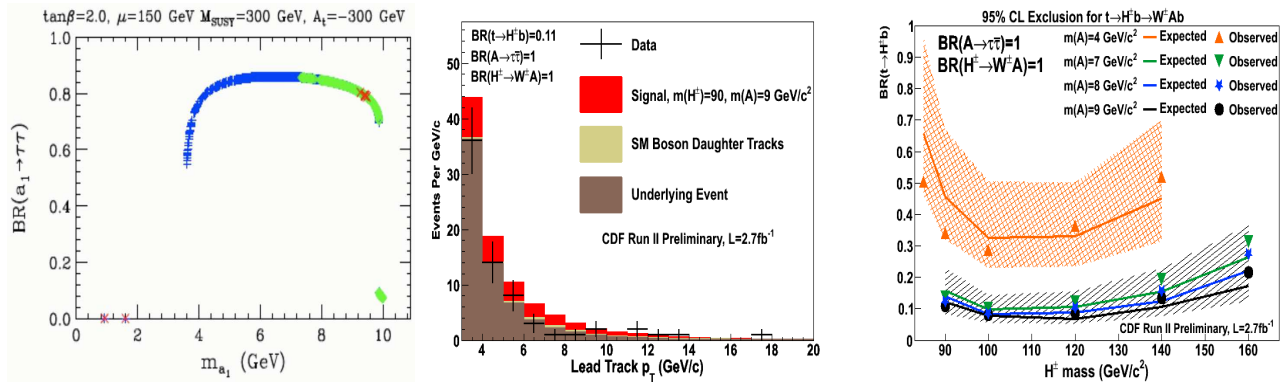


Figure 37. CDF. Left: $BR(A \rightarrow \tau^+ \tau^-)$ for $\tan \beta = 2$ and a particular choice of NMSSM parameters. Center: leading track p_T . Right: $BR(t \rightarrow H^+ b)$ limit at 95% CL for $BR(H^+ \rightarrow W^+ A) = 1$ and $BR(A \rightarrow \tau^+ \tau^-) = 1$ in the NMSSM.

10.4. $H \rightarrow \gamma\gamma$

In fermiophobic Higgs boson models, the dominant decay mode could be $H \rightarrow \gamma\gamma$. The Higgs boson could be produced in the associated production with a vector boson and vector boson fusion (VBF) production mechanisms. No indication of such reactions have been observed and limits are set as shown in Fig. 38 from CDF (left plot from [66]) and from $D\bar{0}$ (center and right plots from [67]).

10.5. H^{++}

The possibility of doubly-charged Higgs boson exists in models with Higgs boson triplets. Pairs of like-sign charged leptons are expected from the decay of the doubly-charged Higgs bosons.

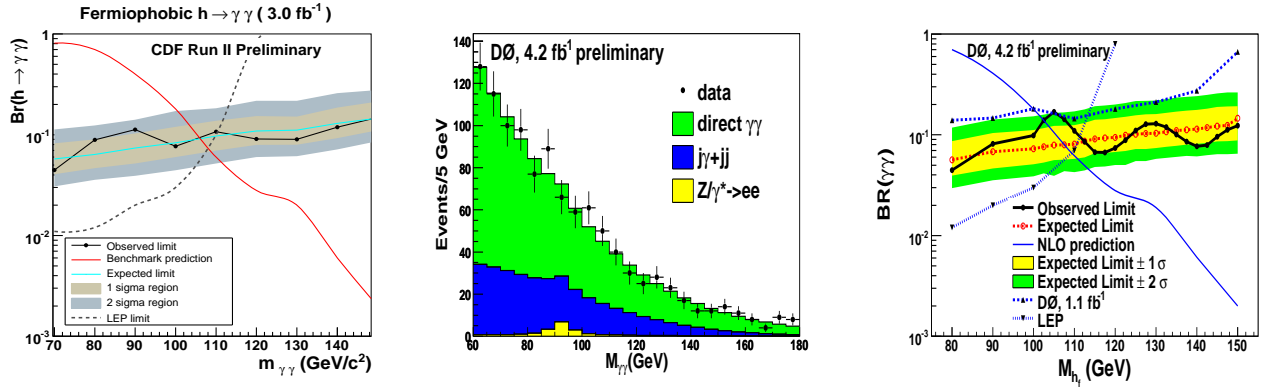


Figure 38. Fermiophobic Higgs. $H \rightarrow \gamma\gamma$. Left: CDF limits at 95% CL. Center: DØ invariant $\gamma\gamma$ mass distribution. Right: DØ limits at 95% CL.

No indication has been observed in the data. The di-muon mass spectrum and limits on the doubly-charged Higgs boson mass are shown in Fig. 39 from CDF (left plot from [68]) and from DØ (center and right plots from [69]).

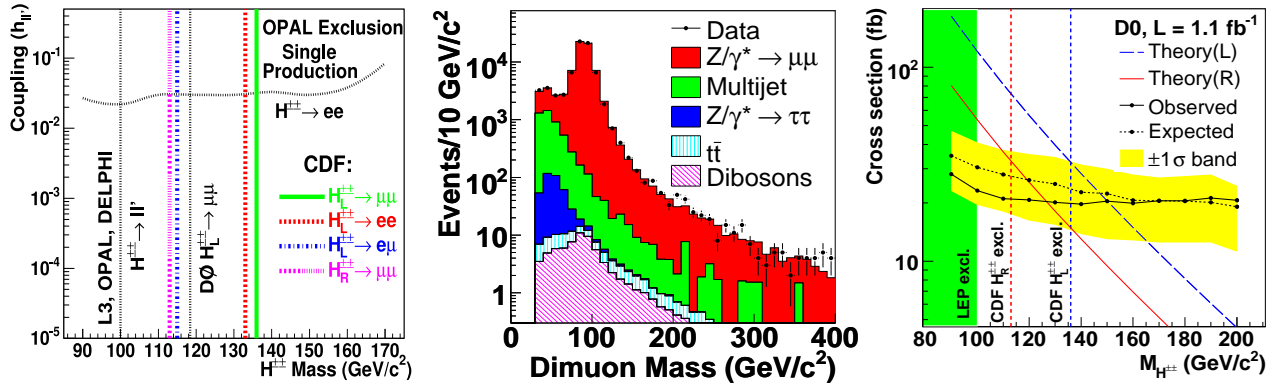


Figure 39. Left: CDF doubly-charged Higgs boson mass limits at 95% CL. Center: DØ di-muon mass spectrum. Right: DØ doubly-charged Higgs boson mass limits at 95% CL.

11. Conclusions

Much has been learned from the searches for Higgs bosons at LEP. The Tevatron Run-II searches for Higgs bosons are well under way and already have set several limits exceeding some previous LEP limits. For the SM Higgs boson, searches for gluon fusion with WW decays, associated production of WH with $b\bar{b}$ and WW decays, and ZH $\rightarrow \nu\bar{\nu}b\bar{b}$, $l^+l^-b\bar{b}$ decays have been performed previously. Updates of these searches have been reported and compared to previous reports with results from summer 2005 and winter 2008/9 [4, 5]. Beyond the Standard Model, the searches at the Tevatron for $b\bar{b}A$, H^+ , H^{++} , $h \rightarrow \gamma\gamma$ and $\tau^+\tau^-$ have led to new limits on couplings and masses. The close collaboration of phenomenologists and experimentalists is crucial to fully exploit the potential of the collected data. The sensitivity of the SM Higgs searches is evolving rapidly, significantly faster than the increase in sensitivity from improved statistics alone. The first direct SM exclusion beyond the LEP results was achieved at high mass, around 165 GeV, in summer 2008. Incorporating the ongoing improvements and analysing the data taken in 2010, an exclusion at 95% CL over virtually the full mass range favoured by the electroweak fits is achievable. In addition three sigma evidence will be possible over much of the same range.

Acknowledgments

I would like to thank my colleagues from the CDF and DØ Higgs working groups for discussions and comments, and the organizers of iNExT'10 conference for their invitation and hospitality.

References

- [1] A. Sopczak, Higgs Physics: From LEP to a Future Linear Collider, Proceedings QFTHEP'04, St. Petersburg, Russia; and WONP'05, Havana, Cuba, hep-ph/0502002, and references therein.
- [2] A. Sopczak, MSSM Higgs boson searches at LEP, presented at the 13th International Conference on Supersymmetry and Unification of Fundamental Interactions (SUSY'05), Durham, UK, July 18-23, 2005, hep-ph/0602136.
- [3] The LEP Electroweak Working Group, <http://lepewwg.web.cern.ch/LEPEWWG> (2010).
- [4] A. Sopczak, Status of Higgs Boson Searches at the Tevatron, arXiv:0903.4312. FERMILAB-CONF-09-088-E-PPD-T, March 2009. Presented at WONP'09 conference, Havana, Cuba, February 9-12, 2009.
- [5] A. Sopczak, New Physics Searches at the Tevatron and the LHC, hep-ph/0605236. FERMILAB-CONF-06-134-E-T, May 2006. Presented at Aspen Summer Workshop on Collider Physics: From the Tevatron to the LHC to the Linear Collider, Aspen, Colorado, August 15 - September 11, 2005.
- [6] CERN and Fermilab experiments, Boson Cross-section Measurements; see also talk by E. Chabalina, ICHEP'10.
- [7] T. Aaltonen et al., CDF Collaboration, Strong Evidence for ZZ Production in $p\bar{p}$ Collisions at $\sqrt{s} = 1.96$ TeV, Phys. Rev. Lett. **100**, 201801 (2008).
- [8] V.M. Abazov et al., DØ Collaboration, Observation of ZZ Production in $p\bar{p}$ Collisions at $\sqrt{s} = 1.96$ TeV, Phys. Rev. Lett. **101**, 171803 (2008).
- [9] Fermilab Operations, <http://www-bdnew.fnal.gov/operations/lum/lum.html> (September 17, 2010).
- [10] F. Maltoni et al. in TeV4LHC Workshop, Standard Model Higgs cross sections at hadron colliders, Fermilab, Chicago, October 2005, hep-ph/0612172.
- [11] A. Djouadi, J. Kalinowski and M. Spira, HDECAY: A program for Higgs boson decays in the Standard Model and its supersymmetric extension, Comput. Phys. Commun. **108**, 56 (1998).
- [12] C.S. Hill, CDF Collaboration, L00: Operational Experience and Performance of the CDFII Silicon Detector, Nucl. Instrum. Meth. **A 530**, 1 (2004).
- [13] DØ Collaboration, R. Lipton, private communications (2009).
- [14] I. Iashvili in TeV4LHC Workshop, Tevatron-for-LHC Report: Higgs, Fermilab, Chicago, October 2005. hep-ph/0612172, and updated plot.
- [15] A. Haas, A Search for Neutral Higgs Bosons at High $\tan\beta$ in Multi-jet Events from $p\bar{p}$ Collisions at $\sqrt{s} = 1960$ GeV, University of Washington, PhD Thesis (2005).
- [16] J. Donini et al., Energy calibration of b-quark jets with $Z \rightarrow b\bar{b}$ decays at the Tevatron Collider, Nucl. Instrum. Meth. **A 596**, 354 (2008).
- [17] T. Altonen et al., CDF Collaboration, Measurement of Cross Sections for b Jet Production in Events with a Z Boson in $p\bar{p}$ Collisions at $\sqrt{s} = 1.96$ TeV, Phys. Rev. **D 79** 052008 (2009).
- [18] V.M. Abazov et al., DØ Collaboration, A Measurement of the Ratio of Inclusive Cross Sections $p\bar{p} \rightarrow Zb/p\bar{p} \rightarrow Zj$ at $\sqrt{s} = 1.96$ TeV, Phys. Rev. Lett. **94**, 161801 (2005).
- [19] DØ Collaboration, Search for Higgs production in dilepton plus missing energy final states with 3.0–4.2 fb^{-1} of $p\bar{p}$ collisions at $\sqrt{s} = 1.96$ TeV, DØ note 5871, March 6, 2009.
- [20] DØ Collaboration, Search for Higgs production in electron and muon plus missing transverse energy final states with 6.7 fb^{-1} of $p\bar{p}$ collisions at $\sqrt{s} = 1.96$ TeV, DØ note 6082, Juli 20, 2010;
DØ Collaboration, Search for Higgs boson production in dilepton and missing energy final states with 5.4 fb^{-1} of $p\bar{p}$ collisions at $\sqrt{s} = 1.96$ TeV, Phys. Rev. Lett. **104**, 061804 (2010);
DØ Collaboration, A search for the standard model Higgs boson $H \rightarrow WW \rightarrow \text{leptons} + \text{jets}$ in 5.4 fb^{-1} of $p\bar{p}$ collisions at $\sqrt{s} = 1.96$ TeV, DØ note 6095, July 21, 2010.
- [21] CDF Collaboration, Search for $H \rightarrow WW^*$ Production at CDF Using 5.9 fb^{-1} of Data, CDF note 10232, August 16, 2010.
- [22] CDF Collaboration, Search for Standard Model Higgs Boson Production in Association with a W Boson

- Using Matrix Element Techniques with 5.6 fb^{-1} of CDF Data, CDF note 10217, July 9, 2010;
 CDF Collaboration, Search for Standard Model Higgs boson production in association with a W boson using Neural Network techniques with 5.7 fb^{-1} , CDF note 10239, July 14, 2010.
- [23] DØ Collaboration, Search for WH associated production with 5.3 fb^{-1} of Tevatron data, DØ note 6092, July 21, 2010.
- [24] DØ Collaboration, Search for Associated Higgs Boson Production with Like-Sign Leptons in $p\bar{p}$ Collisions at $\sqrt{s} = 1.96 \text{ TeV}$, DØ note 6091, July 20, 2010.
- [25] CDF Collaboration, A Search for the Standard Model Higgs Boson in the Process $ZH \rightarrow \ell^+ \ell^- b\bar{b}$ Using 5.7 fb^{-1} of CDF II Data, CDF note 10235, July 16, 2010;
 CDF Collaboration, A Search for the Standard Model Higgs boson in the process $ZH ZH \rightarrow \ell^+ \ell^- b\bar{b}$ using a loosened muon selection, CDF note 10221, July 16, 2010.
- [26] DØ Collaboration, Search for $ZH \rightarrow \ell^+ \ell^- b\bar{b}$ production in 6.2 fb^{-1} of $p\bar{p}$ collisions, DØ note 6089, July 20, 2010.
- [27] CDF Collaboration, Search for the Standard Model Higgs boson in the \cancel{E}_T plus jets sample, CDF note 10212, July 7, 2010 and public web page, July 2, 2010,
http://www-cdf.fnal.gov/physics/new/hdg/Results_files/results/vhmetbb_100705/.
- [28] DØ Collaboration, Search for the standard-model Higgs boson in the $ZH \rightarrow \nu\bar{\nu} b\bar{b}$ channel in 6.4 fb^{-1} of $p\bar{p}$ collisions at $\sqrt{s} = 1.96 \text{ TeV}$, DØ note 6087, August 30, 2010.
- [29] CDF Collaboration, Search for a low mass Standard Model Higgs boson in the $\tau\tau$ decay channel, CDF note 10133, July 9, 2010.
- [30] V.M. Abazov et al., DØ Collaboration, Search for the standard model Higgs boson in tau final states, Phys. Rev. Lett. **102**, 251801 (2009);
 DØ Collaboration, Search for the standard model Higgs boson in the $\tau^+ \tau^- q\bar{q}$ final state, DØ note 5845, August 14, 2009.
- [31] CDF Collaboration, Search for a SM Higgs Boson with the Diphoton Final State at CDF, CDF note 10065, February 23, 2010 and public web page, February 4, 2010,
http://cdfsam-prd.fnal.gov/physics/new/hdg/Results_files/results/hgamgam_jan10/.
- [32] DØ Collaboration, Search for the Standard Model Higgs Boson in $\tau\tau$ final states at DØ with $L = 4.2 \text{ fb}^{-1}$ data, DØ note 5858, February 24, 2009.
- [33] S. Lai, Search for Standard Model Higgs Boson Produced in Association with a Top-Antitop Quark Pair in 1.96 TeV Proton-Antiproton Collisions, University of Toronto, CDF note 9508, PhD Thesis (2006);
 A. Anastassov et al. CDF and DØ Collaborations, Searches for Higgs bosons at the Tevatron, AIP Conf. Proc. **903**, 73 (2007).
- [34] DØ Collaboration, Search for the Standard Model Higgs boson in the $t\bar{t}H \rightarrow t\bar{t}b\bar{b}$ channel, DØ note 5739, March 14, 2009.
- [35] CDF and DØ Collaborations, Combined CDF and DØ Upper Limits on Standard Model Higgs-Boson Production with up to 4.2 fb of Data, CDF note 9713, DØ note 5889, March 12, 2009.
- [36] CDF and DØ Collaboration, Combined CDF and DØ Upper Limits on Standard Model Higgs-Boson Production with up to 6.7 fb^{-1} of Data, CDF note 10241, DØ note 6082, FERMILAB-CONF-10-257-E, July 28, 2010.
- [37] CDF Collaboration, A search for the Higgs Boson in the All Hadronic Channel with Data Sample of 4 fb^{-1} , CDF note 10010, February 3, 2010.
- [38] CDF Collaboration, Search for $H \rightarrow WW$ Production at CDF Using 3.0 fb^{-1} of Data, CDF note 9500, July 25, 2008, and update Moriond'09.
- [39] CDF Collaboration, Search for Standard Model Higgs Boson Production in Association with a W Boson Using Matrix Element and Boosted Decision Tree Techniques with 2.7 fb^{-1} of Data, CDF note 9463, Januar 29, 2009;
 CDF Collaboration, Search for Standard Model Higgs Boson Production in Association with W^\pm Boson at CDF with 2.7 fb^{-1} , CDF note 9468, August 1, 2008;
 CDF Collaboration, Combined $WH \rightarrow \ell\nu b\bar{b}$ search with 2.7 fb^{-1} of CDF data, CDF note 9596, November 19, 2008.
- [40] DØ Collaboration, Search for WH associated production using a combined Neural Network and Matrix Element Approach with 2.7 fb^{-1} of Run II data, DØ note 5828, February 5, 2009.
- [41] CDF Collaboration, Search for the WH Production Using High-pt Isolated Like-Sign Dilepton Events in

- Run II, CDF note 7307, December 19, 2008.
- [42] DØ Collaboration, Search for Associated Higgs Boson Production with Like Sign Leptons in $p\bar{p}$ Collisions at $\sqrt{s} = 1.96$ TeV, DØ note 5873, March 13, 2009.
- [43] CDF Collaboration, A Search for $ZH \rightarrow l^{+1}l^{-}b\bar{b}$ in 2.7 fb^{-1} using a Neural Network discriminant, CDF note 9665, December 11, 2008.
- [44] DØ Collaboration, Search for $ZH \rightarrow e^{+}e^{-}b\bar{b}$ and $ZH \rightarrow \mu^{+}\mu^{-}b\bar{b}$ Production in 4.2 fb^{-1} of data with the DØ Detector in $p\bar{p}$ Collisions at $\sqrt{s} = 1.96$ TeV, DØ note 5876, March 12, 2009.
- [45] CDF Collaboration, Search for the Standard Model Higgs boson in the \cancel{E}_T plus jets sample, CDF note 9642, December 29, 2008 and public web page, December 15, 2008, http://www-cdf.fnal.gov/physics/new/hdg/results/vhmetbb_081107/.
- [46] DØ Collaboration, Search for the standard model Higgs boson in the $HZ \rightarrow b\bar{b}\nu\bar{\nu}$ channel in 2.1 fb^{-1} of $p\bar{p}$ collisions at $\sqrt{s} = 1.96$ TeV, DØ note 5586, February 29, 2008.
- [47] CDF Collaboration, Search for the Standard Model Higgs Boson in $H \rightarrow \tau\tau$ Channel at CDF Run II – Simultaneous Search for WH/ZH/VBF/H Processes, CDF note 9248, February 22, 2008.
- [48] DØ Collaboration, Search for the standard model Higgs boson in τ final states, DØ note 5883, March 9, 2009.
- [49] CDF Collaboration, Search for a Fermiophobic Higgs Boson with the Diphoton Final State at CDF, CDF note 9586, October 29, 2008.
- [50] CDF and DØ Collaborations, “Projections”, <http://www-cdf.fnal.gov/physics/new/hdg/results> (2010).
- [51] J. Campbell, R. K. Ellis, F. Maltoni and S. Willenbrock, Higgs Boson Production in Association with a Single Bottom Quark, *Phys. Rev. D* **67**, 095002 (2003).
- [52] S. Dawson, C. B. Jackson, L. Reina and D. Wackerroth, Exclusive Higgs boson production with bottom quarks at hadron colliders, *Phys. Rev. D* **69**, 074027 (2004);
S. Dittmaier, M. Krämer and M. Spira, Higgs radiation off bottom quarks at the Fermilab Tevatron and the CERN LHC, *Phys. Rev. D* **70**, 074010 (2004).
- [53] V.M. Abazov et al., DØ Collaboration, Search for neutral supersymmetric Higgs bosons in multijet events at $\sqrt{s} = 1.96$ TeV, *Phys. Rev. Lett.* **95**, 151801 (2005).
- [54] CDF Collaboration, Search for Higgs Bosons Produced in Association with b-Quarks, CDF note 10105, June 13, 2010.
- [55] DØ Collaboration, Search for neutral Higgs bosons in multi-b-jet events in $p\bar{p}$ collisions at $\sqrt{s} = 1.96$ TeV, DØ note 5726, July 25, 2008.
- [56] CDF Collaboration, Search for Neutral MSSM Higgs Bosons Decaying to Tau Pairs with 1.8 fb^{-1} of Data, CDF note 9071, October 22, 2007;
T. Aaltonen et al., CDF Collaboration, Search for Higgs Bosons Predicted in Two-Higgs-Doublet Models via Decays to Tau Lepton Pairs in 1.96 TeV $p\bar{p}$ Collisions, *Phys. Rev. Lett.* **103**, 201801 (2009).
- [57] DØ Collaboration, Search for MSSM Higgs Boson Production in the Decay $h \rightarrow \tau_{\mu}\tau_{\text{had}}$ with the DØ Detector at $\sqrt{s} = 1.96$ TeV, DØ note 5728, July 25, 2008;
DØ Collaboration, Search for MSSM Higgs Boson Production in Di-tau Final States with $L=2.2 \text{ fb}^{-1}$ at the DØ Detector, DØ note 5740, July 29, 2008.
- [58] CDF and DØ Collaborations, Combined CDF and DØ upper limits on MSSM Higgs boson production in tau-tau final states with up to 2.2 fb^{-1} of data, CDF note 10099, DØ note 6036, arXiv:1003.3363, FERMILAB-FN-0851-E, March 22, 2010.
- [59] DØ Collaboration, Search for charged Higgs bosons in $t\bar{t}$ quark decays, DØ note 5715, July 28, 2008;
V.M. Abazov, et al., DØ Collaboration, Search for charged Higgs bosons in top quark decays, *Phys. Lett. B* **682**, 278 (2009).
- [60] A. Abulencia et al., CDF Collaboration, Search for Charged Higgs Bosons from Top Quark Decays in $p\bar{p}$ Collisions at $\sqrt{s} = 1.96$ TeV, *Phys. Rev. Lett.* **96**, 042003 (2006).
- [61] V.M. Abazov, DØ Collaboration, Simultaneous Measurement of the Ratio $R = B(t \rightarrow Wb)/B(t \rightarrow Wq)$ and the Top-Quark Pair Production Cross Section with the DØ Detector at $\sqrt{s} = 1.96$ TeV, *Phys. Rev. Lett.* **100**, 192003 (2008);
DØ Collaboration, Measurement of the $t\bar{t}$ Production cross section at $\sqrt{s} = 1.96$ TeV in Dilepton Final States Using 1 fb^{-1} , DØ note 5371, March 13, 2007;
DØ Collaboration, Measurement of the Cross Section Ratio $\sigma(p\bar{p} \rightarrow t\bar{t})_{\ell+\text{jets}}/\sigma(p\bar{p} \rightarrow t\bar{t})_{\ell\ell}$ with the DØ Detector at $\sqrt{s} = 1.96$ TeV in the Run II Data, DØ note 5466, August 14, 2008.

- [62] CDF Collaboration, A search for charged Higgs in lepton + jets $t\bar{t}$ events using 2.2 fb⁻¹ of CDF data, CDF note 9322, May 12, 2008;
T. Aaltonen, et al., CDF Collaboration, Search for charged Higgs bosons in decays of top quarks in $p\bar{p}$ collisions at $\sqrt{s} = 1.96$ TeV, Phys. Rev. Lett. **103**, 101803 (2009).
- [63] V.M. Abazov, et al., DØ Collaboration, Search for Charged Higgs Bosons Decaying into Top and Bottom Quarks in $p\bar{p}$ Collisions, Phys. Rev. Lett. **102**, 191802 (2009).
- [64] R. Dermisek and J. Gunion, Many light Higgs bosons in the next-to-minimal supersymmetric model, Phys. Rev. **D 79** 055014 (2009).
- [65] CDF Collaboration, Search for Light Higgs Boson from Top Quark Decays, CDF note 10104, June 7, 2010;
T. Aaltonen et al., CDF Collaboration, Measurement of the Ratio $\sigma_{t\bar{t}}/\sigma_{Z/\gamma^* \rightarrow \ell\ell}$ and Precise Extraction of the $t\bar{t}$ Cross Section, Phys. Rev. Lett. **105**, 012001 (2010).
- [66] CDF Collaboration, Search for a Fermiophobic Higgs Boson with the Diphoton Final State at CDF, CDF note 9586, October 30, 2008.
- [67] DØ Collaboration, Search for a Fermiophobic Higgs Boson in the diphoton final state using 4.2 fb⁻¹ of DØ data, DØ note 5880, March 11, 2009.
- [68] D. Acosta et al., CDF Collaboration, Search for Long-Lived Doubly Charged Higgs Bosons in $p\bar{p}$ Collisions at $\sqrt{s} = 1.96$ TeV, Phys. Rev. Lett. **95**, 071801 (2005).
- [69] V.M. Abazov et al., DØ Collaboration, Search for Pair Production of Doubly Charged Higgs Bosons in the $H^{++}H^{--} \rightarrow \mu^+\mu^+\mu^-\mu^-$ Final State, Phys. Rev. Lett. **101**, 071803 (2008).